EUROPEAN JOURNAL OF ENTOMOLOGY
ISSN (online): 1802-8829
http://www.eje.cz
Eur. J. Entomol. **115**: 535–561, 2018
doi: 10.14411/eje.2018.053
ORIGINAL ARTICLE

Larval descriptions of five Oriental bamboo-inhabiting *Acroceratitis* species (Diptera: Tephritidae: Dacinae) with notes on their biology

Alexander SCHNEIDER[1], Damir KOVAC[1], Gary J. STECK[2] and Amnon FREIDBERG[3]

[1] Forschungsinstitut Senckenberg, Senckenberganlage 25, D-60325 Frankfurt am Main, Germany; e-mails: alexander.schneider@senckenberg.de, damir.kovac@senckenberg.de

[2] Florida State Collection of Arthropods, Florida Department of Agriculture & Consumer Services, Gainesville, FL 32614-7100, U.S.A.; e-mail: gary.steck@freshfromflorida.com

[3] The Steinhardt Museum of Natural History, Israel National Center for Biodiversity Studies, Department of Zoology, George S. Wise Faculty of Life Sciences, Tel Aviv University, Tel Aviv 69978, Israel; e-mail: afdipter@post.tau.ac.il

Key words. Tephritidae, Gastrozonini, *Acroceratitis*, first description, larvae, morphology, biology, Poaceae, bamboo, Thailand

Abstract. Third instar larvae of the genus *Acroceratitis* Hendel from North Thailand are described for the first time. They belong to *A. ceratitina* (Bezzi), *A. distincta* (Zia), *A. histrionica* (de Meijere), *A. incompleta* Hardy, and *A. septemmaculata* Hardy. Short descriptions of eggs, empty egg shells, and puparia are also presented. *Acroceratitis* larvae infest shoots of bamboo (Poaceae). Larval host plants of the studied species are *Bambusa polymorpha* Munro, *Cephalostachyum pergracile* Munro, *Dendrocalamus hamiltoni* Nees and Arnott ex Munro, *D. strictus* (Roxbourgh), *Dendrocalamus* sp. (unidentified) and *Pseudoxytenanthera albociliata* (Munro). The morphological characters of *Acroceratitis* larvae are compared with those of other Gastrozonini described so far. A key to *Acroceratitis* larvae is provided. *Acroceratitis ceratitina*, *A. incompleta* and *A. septemmaculata* are morphologically similar and clearly differentiated from *A. distincta* and *A. histrionica* by the lack of additional papillar sensilla on the labial lobe, the arrangement of the spinules on the creeping welts and other characters. The morphological differences between the two groups coincide with the type of substrate utilized by their larvae: *A. ceratitina*, *A. incompleta* and *A. septemmaculata* larvae feed in young and soft internode walls, while *A. distincta* and *A. histrionica* utilize harder bamboo tissue of already elongated bamboo shoot internodes. *Acroceratitis histrionica* larvae are special within the Gastrozonini, because they develop exclusively in cavities formed by the internode surface and the protecting culm sheath. Factors influencing spatial utilization of larval resources, preference for upright shoots as breeding substrate, larval behavior, types of bamboo damage caused by different species and attraction to sweat and urine in the adults are discussed.

INTRODUCTION

Acroceratitis Hendel is a genus of the tribe Gastrozonini, subfamily Dacinae (Korneyev, 1999) comprising 17 described species (Kovac et al., 2006; David et al., 2014). Most Dacinae are frugivorous and many are pests of commercially important fruits and vegetables (White & Elson-Harris, 1992). In contrast, Gastrozonini (and a few Acanthonevrini, subfamily Phythalmiinae) are the only tephritids feeding on Poaceae. The larvae of the Asian Gastrozonini develop in bamboo shoots (Bambusoidea), whereas species of the three African genera are associated with other grasses [*Hyparrhenia cymbaria* (L.) Stapf, *Panicum maximum* Jacq., *Pennisetum polystachyon* (L.) Schult, and *Sporobolus pyramidalis* P. Beauv.] (Allwood et al., 1999; Hancock, 1999; Kovac et al., 2006; Copeland, 2007; Dohm et al., 2014).

So far, larvae of only six Gastrozonini species have been known: Elson-Harris (1992) described the third instar larvae of *Chaetellipsis paradoxa* Bezzi (as *Chaetellipsis atrata* Hardy), *Chaetellipsis maculosa* Hancock and Drew (as *Chaetellipsis* sp. n.; see Hancock & Drew, 1999), *Gastrozona fasciventris* (Macquart) and *Cyrtostola limbata* (Hendel) [as *Taeniostola limbata* (Hendel); see Hancock & Drew, 1999], while Kovac et al. (2013, 2017) described the third instar larvae of *Ichneumonopsis burmensis* (Hardy) and *Acrotaeniostola spiralis* Munro.

In the present study we describe the third instar larvae of *Acroceratitis ceratitina* (Bezzi), *A. distincta* (Zia), *A. histrionica* (Meijere), *A. incompleta* Hardy, and *A. septemmaculata* Hardy, all collected by D. Kovac in North Thailand. Brief descriptions of the puparia of the five species as well as the eggs of *A. histrionica* are presented. The larval characters of *Acroceratitis* species are compared with previously described Gastrozonini larvae. An overview of the hitherto largely unknown habitat and biology of the examined *Acroceratitis* species is given.

MATERIAL AND METHODS

Study site

Field work was conducted in North Thailand (Province Mae Hong Son) in the mountainous Pangmapha district. Pangmapha has three distinct seasons, the rainy season (mid May to mid October), the cool season (mid October to mid February) and the hot season (mid February to mid May). The daytime temperatures rise up to 35–37°C in March/April with peaks above 40°C. In December/January it is cool at night, when the temperatures drop to around 13°C or lower depending on the elevation. Annual rainfall varies from 1100 to 1500 mm with the peak at the end of the monsoon period in August/September (Müller, 1996; Gardner et al., 2000). Bamboo host plants of *Acroceratitis* species were common in farming areas at elevations between 600 and 1600 m. Collecting took place between 2010 and 2017. Each year field work was conducted during two periods leaving only the months January and February unsampled.

Collecting, rearing and preservation

Flies were collected by sweeping over bamboo (shoot surface, leaves) or the surrounding vegetation. Larvae were obtained by cutting off pieces of infested bamboo shoots. Infested shoots were recognized by the withered sheaths and blades occurring at the apex of shoots. Shoots were also cut randomly in order to find larvae in seemingly undamaged shoots. Another method for obtaining larvae was to cut bamboo shoots, place them on the ground or in the upright position and check about 2 weeks later if they were infested by tephritid larvae.

Bamboo shoot sections containing tephritid larvae were transported to the lab in plastic bags. In the lab larvae were grouped according to their size and colour and kept in separate plastic rearing containers at room temperature. Rearing containers were provided with original shoot substrate and were covered with fine-mesh gauze. They were checked daily and substrate moistened if necessary. If larvae from the same container developed different characters (color, size), indicating a mixture of two or more species, they were separated from each other. Mature larvae left their substrate for pupariation and were then transferred to smaller plastic containers and allowed to pupariate between moistened paper tissues.

For preservation, some *Acroceratitis* larvae were immersed in boiling water for 2–3 min in order to kill them and keep their cuticle pale and expanded. The larvae were eventually transferred to 70% ethanol for permanent storage. Three days after eclosion the adults were killed with ethyl acetate and pinned or transferred to 70% ethanol. Some adults and unboiled larvae were preserved in absolute ethanol.

Slide mounting

For the study of the cephalopharyngeal skeleton and the posterior spiracles, the preserved larvae were cut transversely in three parts. The first cut was set between the thorax and the abdomen and the second between the 7th and 8th abdominal segment. The anterior body part (containing the cephalopharyngeal skeleton) and the posterior body part (containing the posterior spiracles) were macerated overnight in 10% potassium-hydroxide (KOH) solution at room temperature, following the method used by Steck & Wharton (1986) and Steck et al. (1990). Subsequently the cephalopharyngeal skeleton was further cleared at 60°C in 10% KOH for about 1.5 h. The macerated larval parts were washed in distilled water for 1 h in order to remove the KOH. Then, they were dehydrated in 80% and 96% ethanol and finally transferred to terpineol for 15 min each. Finally, the cephalopharyngeal skeleton and the posterior spiracles were slide-mounted in Canada balsam, still enclosed by the transparent larval cuticle.

Scanning electron microscopy (SEM)

Larvae were cut in three parts as described above but the first cut was set between the first and second and the second cut was set between the fifth and sixth abdominal segment. The larval body parts were washed in 80% ethanol three times in order to remove body substances leaking out of the cuts, dehydrated in 96% ethanol for one hour, transferred to hexamethyldisilazane (HMDS; Nation, 1983) for one hour, and subsequently transferred to fresh HMDS for one additional hour. Subsequently, HMDS containing the specimens was allowed to evaporate under a fume hood. Dried specimens were mounted on stubs, coated with gold-palladium and observed under a Hitachi scanning electron microscope (CamScan CS24).

Terminology

Terminology follows White et al. (1999). The term "pseudocephalon" is used according to Courtney et al. (2000). Isolated sensilla were named according to Frías et al. (2006), Frías Lasserre et al. (2009), and Kovac et al. (2013, 2017).

The general description provided below applies to all species. Thereafter *A. ceratitina* is described in detail, while for *A. incompleta*, *A. septemmaculata* and *A. distincta* only their differences from *A. ceratitina* are noted; similarly for *A. histrionica* only its further differences from *A. distincta* are noted.

The examined material is stored in the collection of the Senckenberg Forschungsinstitut, Frankfurt am Main.

RESULTS

Diagnosis of larval Gastrozonini

Third instar larvae of the tribe Gastrozonini share several characters with other tribes of the subfamily Dacinae (Ceratidini and Dacini). These are the ability to jump (exception: *Ichneumonopsis burmensis*), presence of caudal ridges (exception: *Acrotaeniostola spiralis* and *Ichneumonopsis burmensis*), dark transverse line on caudal segment (exception: *Acrotaeniostola spiralis* and *Ichneumonopsis burmensis*), similarly shaped preoral lobes, and a preapical tooth on mouthhooks (Carroll, 1992; Elson-Harris, 1992; Kovac et al., 2013, 2017). Gastrozonini are distinguished from Dacini and Ceratitini by the lack of dental sclerites which are according to Carroll (1992) a synapomorphy of Dacini and Ceratitini.

Since none of the morphological characters characterizing Gastrozonini species as Dacinae are present in all Gastrozonini species, the easiest way to discriminate Gastrozonini larvae from other Tephritidae is to include their association with Poaceae as a diagnostic character. This also applies to adult flies (Kovac et al., 2006). The only other tephritids breeding in grasses belong to the tribe Acanthonevrini (Phytalmiinae) (Allwood et al., 1999; Hancock & Drew, 1999; Dohm et al., 2014). Acanthonevrini larvae can easily be distinguished from Gastrozonini, for example, by their large anal lobes and especially by the typical shape of the facial mask (great number of very long oral ridges; patches of ridges similar to oral ridges anterior to mouth opening) (Elson-Harris, 1992).

Genus *Acroceratitis* Hendel, 1913

Larval description of third instar larvae

Habitus. Anterior end of the body conical, posterior end truncate.

Pseudocephalon. Facial mask approximately triangular. 7–22 rows of serrated oral ridges of medium length. 8–17 short accessory plates lateral to oral ridges covering a much smaller area than oral ridges. Accessory plates most often very similarly serrated as oral ridges but in some cases teeth of accessory plates shorter, wider, and more irregular than those of oral ridges. Antenna and maxillary sense organs located on moderately to well-developed cephalic lobes. Antenna two-segmented. Maxillary sense organ composed of maxillary palpus and a dorsolateral group of sensilla, both lying close to each other. Maxillary palpus surrounded by a complete or incomplete cuticular fold bearing three papillar sensilla and two knob sensilla. Dorsolateral group of sensilla of maxillary sense organ containing two papillar sensilla. Primary preoral lobe rounded to oval, surrounded by 7–13 non-serrated preoral lobes. Preoral organ located on primary preoral lobe, bearing 2–3 peg sensilla. Labial lobe elongate, widened at apex, either entirely smooth or bearing tubercles at base. Labial organ with two openings, with or without two papillar sensilla near these openings. Five pairs of pseudocephalic pit sensilla present: one pair between the antennae, one pair between the maxillary sense organs, one posteroventral to the antenna, and two laterally to the facial mask.

Cephalopharyngeal skeleton. Total length 0.8–1.1 mm. Indentation between apex of apical tooth and ventral apodeme 0.13–0.23× as deep as length of mouthhook (measurements as shown by Frías et al., 2006; Fig. 2). Mouthhooks each bearing one small preapical tooth. Hypopharyngeal sclerite 2.6–5.1× as long as high. Labial sclerite light brown. Pharyngeal sclerite similar to those of other Gastrozonini: brown, darker in area of tentorial phragma and dorsal and ventral bridges; dorsal and ventral bridges protruding. Length of dorsal cornu 0.8–1.1× that of ventral cornu; dorsal cornu cleft; ventral cornu with a bulge on dorsal margin, and with a lighter brown area below this bulge. Parastomal bars light brown, 0.8–1.1× as long as hypopharyngeal sclerite. Anterior sclerite present in all species (but not in all specimens of *A. distincta*).

Thoracic segments. Anterior spiracles with 13–21 approximately cylindrical tubules arranged in a single row. Slit-like opening visible at apex of each tubule. Anterior margin of first thoracic segment covered with numerous rows of dentate plates. Anterior margins of second and third thoracic segments lined with spinules. Third thoracic segment with rudimentary spiracle near its anterior margin. As shown in Fig. 17, isolated sensilla form a similar pattern in all examined *Acroceratitis* species. Each thoracic segment bearing ventrally a pair of Keilin's organs.

Abdominal segments I–VII. As shown in Fig. 17, isolated sensilla similarly distributed in all examined *Acroceratitis* species. Each segment with rudimentary spiracles near anterior margin and with ventral creeping welts which bear rows of spinules in variable arrangements.

Caudal segment. Posterior spiracles somewhat above midline of caudal area, shortest distance between spiracles 0.3–0.9× length of longest opening. Peritreme hyaline; spiracular chamber light brown, spiracular openings surrounded by broad, dark areas, ecdysial scar visible. In caudal view central opening located more lateral than dorsal or ventral opening; angle between dorsal and central opening up to 25°, shortest distance between dorsal and central opening 0.2–0.7× length of longest opening; angle between central and ventral opening up to 33°, shortest distance between central and ventral opening 0.1–0.5× length of the longest opening. Rima visible; spiracular openings 4.0–9.4× as long as wide. Spiracular hairs emerge from small protuberances and are arranged in four groups; hairs branched up to 7×, up to 0.6× as long as longest spiracular opening; dorsal bundle containing 2–20 hairs, ventral bundle containing 5–20 hairs, lateral bundles containing 2–8 hairs.

Caudal ridges and dark transverse line on caudal area present in all species. Area covered by oval anal lobes approximately as long as wide, surrounded by rows of spinules. Sensilla on caudal segment all present and similarly distributed as in other Dacinae (White et al., 1999). A row of three pit sensilla present on each side between anterior margin of anal lobes and lateral sensillum. Creeping welt of caudal segment similar to creeping welts of abdominal segments II–VII.

Diagnosis of third instar larvae

Facial mask triangular, oral ridges regularly to irregularly serrated, accessory plates slightly to distinctly serrated; preoral organ most often bearing three peg-sensilla; preoral lobes non-serrated. Mouthhooks with one preapical tooth. Tubules of anterior spiracle arranged in single row. Creeping welts bearing broad band of very small spinules between two areas covered with posteriorly directed spinules (in *A. histrionica* this band is replaced by 3 to 4 rows of anteriorly directed spinules); anterior margins of abdominal segments at least partly lined with bands or patches of very small spinules. Area covered by both anal lobes approximately as long as wide; anal lobes surrounded by spinules. Spiracular slits surrounded by broad, dark areas.

Biology

In north Thailand *Acroceratitis* adults were found in the field between March and December. During the hot season (March to about mid-May) flies stayed in shady places along streams. At the beginning of the rainy season they dispersed to surrounding bamboo areas. Flies fed on juices oozing from cut bamboo shoots or injured mature culms, dabbed on bamboo extrafloral nectaries, bird droppings, leaves, human urine, human sweat (on backpack, sweeping net, etc.) or imbibed water from vegetation. These food sources provided essential nutrients such as carbohydrates (bamboo nectaries), amino acids, organic acids, sugars (plant exudates) or protein (bird feces) and were also recorded from other tephritids (overview in Drew & Yuval, 2000).

Acroceratitis larvae developed in bamboo shoots of various host species belonging to *Bambusa*, *Cephalostachyum*, *Dendrocalamus*, *Gigantochloa*, *Pseudoxytenanthera* and *Thyrsostachys* (mostly own records, see also Allwood et al., 1999; Dohm et al., 2014). They were oligophagous,

but occupied specific niches regardless of bamboo species. Thus, *A. ceratitina* macerated the apex of thicker shoots just protruding from the soil (Fig. 3A, B), *A. incompleta* and *A. septemmaculata* mined in walls of taller thick shoots ca. 50 cm below the apex (Figs 12A, B, C, 15A, B), *A. histrionica* scraped substrate from the surface of partly hardened internodes located in the lower part of thick and tall shoot stems (Fig. 9A, C, D) and *A. distincta* was confined to thin bamboo shoots or thin side branches of larger shoots (Fig. 6A, C).

Eggs were deposited below the edges of the tough internode sheaths (Figs 6G, 12F, 15E). Freshly hatched larvae squeezed between the sheaths and internode surface towards their feeding sites. Young larvae were milky-colored and pale (Fig. 9C, D), but during growth their colors changed. *A. distincta* and *A. histrionica* became pale yellow and finally bright yellow when mature (Fig. 6D–F). A. *ceratitina*, *A. incompleta* and *A. septemmaculata* became yellow, then yellow-orange and finally spotted orange-green to greenish (Figs 3C and D, 12D, 12E, 15B and C). Mature larvae readily skipped and abandoned their internodes for pupariation in the soil. Larval development took 4–6 weeks.

Key to third instar larvae

1 Anterior spiracle with 14 or fewer tubules; central opening of posterior spiracles up to 5× as long as wide; creeping welts bearing anteriorly directed spinules anteriorly and 2 bands of very small spinules in the middle (Fig. 5D) ..... *A. distincta*
– Anterior spiracles with more than 14 tubules; central opening of posterior spiracles more than 5.3× as long as wide; creeping welts different 2
2 Less than 10 oral ridges; creeping welts with central rows of anteriorly directed spinules (Fig. 8D); distance between posterior spiracles more than 0.6× the length of the longest spiracular opening..... *A. histrionica*
– More than 13 oral ridges; creeping welt with central band of very small spinules (Figs 2D, 11D, 14D); distance between posterior spiracles less than 0.6× the length of the longest spiracular opening..... 3
3 Anal lobes centrally without longitudinal ridges (Fig. 2C); no dentate scales (just posteriorly directed spinules) posterior to anal lobes (Fig. 2C); labial lobe with few, small tubercles at base (Fig. 1E); up to 11 shorter accessory plates (Fig. 1B).... ..... *A. ceratitina*
– Anal lobes centrally with longitudinal ridges (Figs 11C, 14C); dentate scales posterior to anal lobes (Figs 11C, 14C); labial lobe without tubules at base (Figs 10E, 13E); more than 11 accessory plates (Figs 10B, 13B) 4
4 Anterior spiracle with 15 to 16 tubules; dorsal corner of facial mask distinctly pointed; band of accessory plates surrounding the oral ridges strongly widened dorsally, forming the distinctly pointed dorsal corner of the facial mask (Fig. 10B).... ..... *A. incompleta*
– Anterior spiracle with 17 to 19 tubules; dorsal corner of facial mask distinctly rounded; band of accessory plates surrounding the oral ridges of more or less the same width over its entire length (Fig. 13B) ..... *A. septemmaculata*

Acroceratitis ceratitina (Bezzi, 1913)

Stictaspis ceratitina Bezzi, 1913.
Acroceratitis cognata Hardy, 1973.
Cheliophora clavifera Hering, 1938.
Cheliophora gladiella Munro, 1938.
Acroceratitis biseta Wang, 1998.

Description

Habitus. Length: 9.3–9.9 mm (median: 9.6 mm; n = 5); maximum width about 1.5 mm (n = 5). Mature larvae broadest in the area of abdominal segments II–IV.

Pseudocephalon (Fig. 1). Number of serrated oral ridges 19–22. With 9–11 distinctly to slightly serrated accessory plates.

Cephalic lobes well-developed (Fig. 1A). Basal segment of antenna much wider than long, apical segment cone-shaped. Maxillary palpus surrounded by a complete (Fig. 1C) or incomplete cuticular fold.

Primary preoral lobe rounded to oval; preoral lobes 7–9 (Fig. 1D). Preoral organ bearing two to three peg, one papillar, and one pit sensilla. Labial lobe with about five small tubules at base (Fig. 1E). Two papillar sensilla located close to labial organ.

Cephalopharyngeal skeleton (Fig. 16). Total length 1.0–1.1 mm (n = 2). Mouthhooks dark brown, indentation between apex of apical tooth and ventral apodeme 0.18–0.20× as deep as mouthhook length; apical tooth dark brown, curved; neck short; preapical tooth about 0.01 mm long; dorsal apodeme posterodorsally directed; ventral apodeme broad, ventrally directed. Hypopharyngeal sclerite about 3.6× as long as high, anterior part black, posterior part brown. Hypopharyngeal bridge 0.02–0.04 mm long, about 0.03 mm wide, located in the middle of hypopharyngeal sclerite. Dorsal and ventral cornua light brown; ventral cornu with hyaline area at ventral margin and large hyaline area at posterior tip; brown part of dorsal cornu about 0.77× as long as brown part of ventral cornu. Parastomal bars straight, slightly shorter than hypopharyngeal sclerite. Anterior sclerite brown.

Thorax. Anterior spiracles with 18–21 tubules (Fig. 1F). Anterior margin of second and third thoracic segments with 5–7 rows of stout spinules; rows on third thoracic segment with a small gap dorsally.

Abdominal segments I–VII. First abdominal creeping welt bearing a narrow band of very small spinules anteriorly, and about 10 rows of large, stout, posteriorly directed spinules posteriorly; creeping welts of abdominal segments II–VII bearing rows of spinules arranged as follows (from anterior to posterior): A band of very small spinules (sometimes reduced to net-like rows), 7–10 rows of large, stout, posteriorly directed spinules, a band of very small spinules, 4–7 rows of larger, more slender, posteriorly directed spinules (Fig. 2D). Laterally and dorsally, anterior margin of first abdominal segment showing a slender band of very small spinules anteriorly and about 5 rows of large, stout, posteriorly directed spinules posteriorly (rows mediodorsally interrupted); anterior margins of second and third abdominal segment covered laterally with very small spinules anteriorly and about 4 rows of large, stout, posteriorly directed spinules posteriorly. Rows of spinules reaching far dorsally in second abdominal segment, extending somewhat less far dorsally in third abdominal segment. Anterior margins of abdominal segments IV–VII laterally

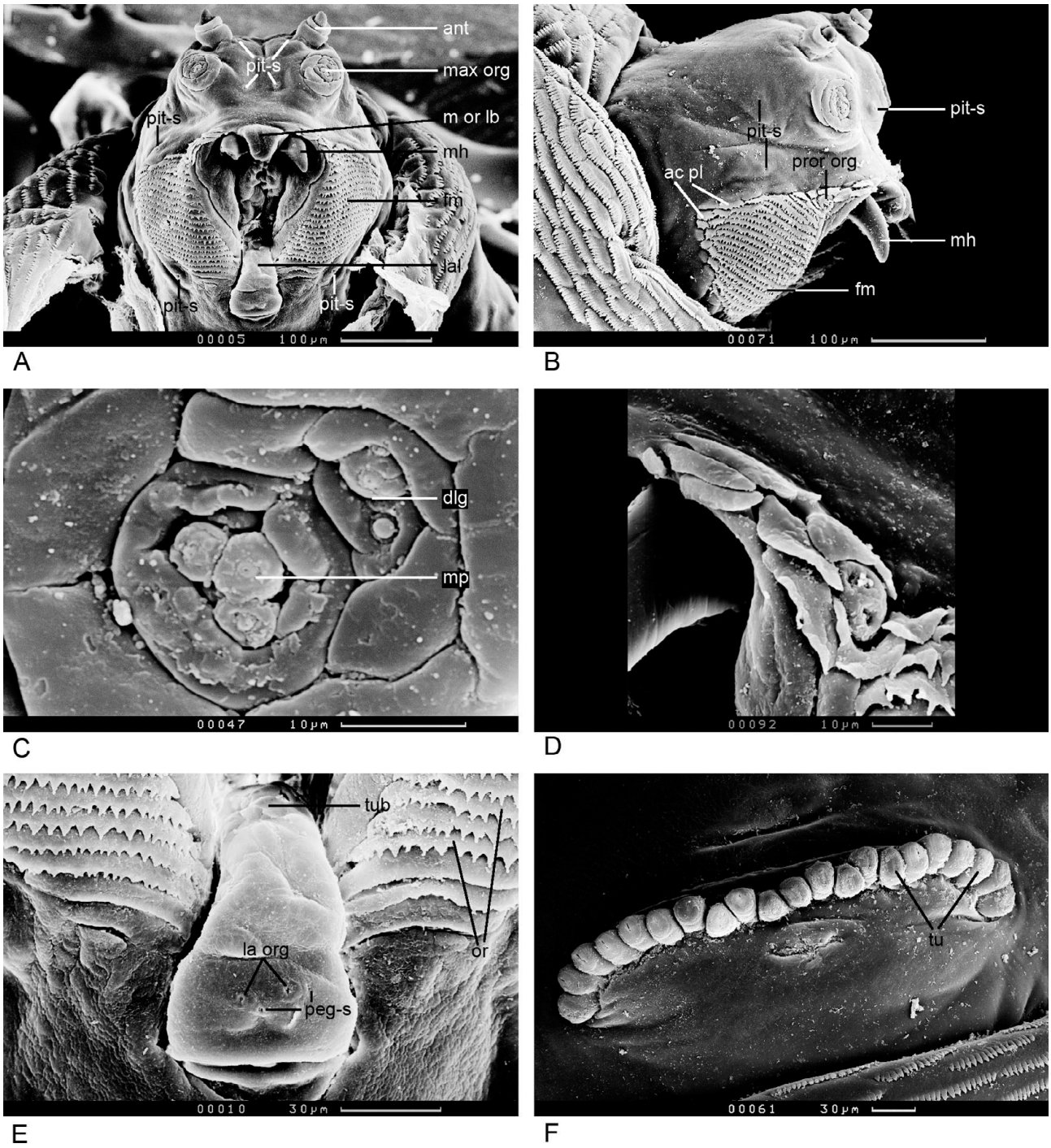

Fig. 1. Pseudocephalon and anterior spiracle of *Acroceratitis ceratitina* (SEM micrographs). A – pseudocephalon, frontal view. B – pseudocephalon and part of the first thoracic segment, lateral view. C – maxillary sense organ. D – preoral organ located on primary preoral lobe, surrounded by remaining preoral lobes. E – labial lobe. F – anterior spiracle. Abbreviations: ant – antenna, dlg – dorsolateral group of sensilla, fm – facial mask, la org – labial organ, lal – labial lobe, m or lb – median oral lobe, max org – maxillary sense organ, mh – mouthhook, mp – maxillary palpus, peg-s – peg sensillum, pit-s – pit sensillum, pror org – preoral organ, tu – tubules, tub – tubercles.

covered by very small spinules, extending less far dorsally than on the respectively more anterior segment.

Caudal segment (Figs 16 and 2A–C). Shortest distance between spiracles about half as long as longest spiracular opening. Angle between dorsal and central opening 1–9°, shortest distance between dorsal and central opening about one third as long as longest opening; angle between central and ventral opening 16–24°, shortest distance between central and ventral opening about 0.15× as long as longest opening. Spiracular openings 6.7–7.8× as long as wide. Spiracular hairs up to 0.4× the length of the longest opening, spiracular hairs branched up to 6×; dorsal bundle containing 10–14 hairs, ventral bundle containing 8–11 hairs, dorsolateral bundle containing 3–5 hairs, ventrolateral bundle containing 4–5 hairs (Figs 16 and 2B).

Anal lobes protuberant. About 2 rows of anteriorly directed spinules anterior to anal lobes and about 5 rows of posteriorly directed spinules posterior to anal lobes (Fig.

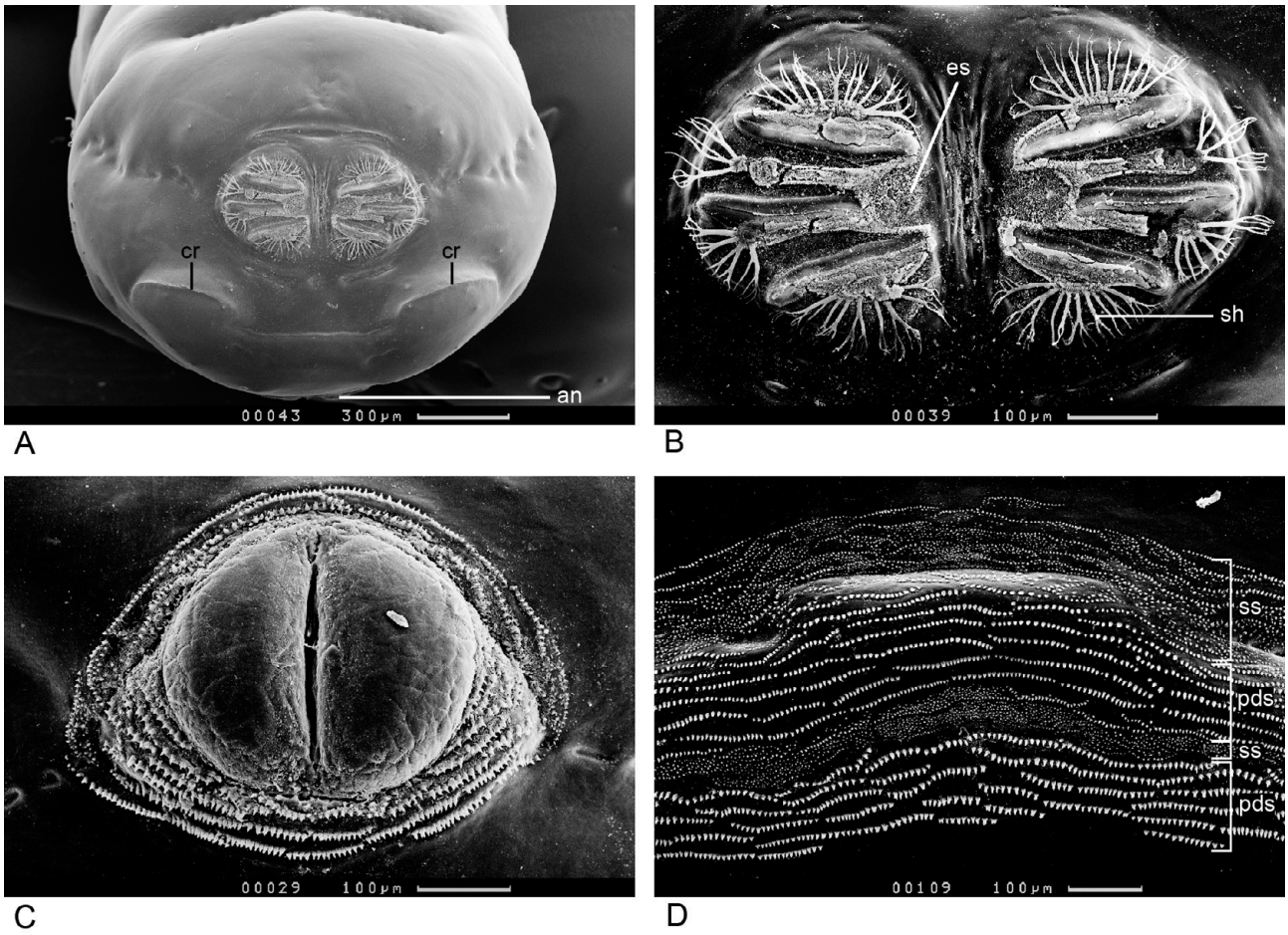

Fig. 2. Creeping welt and caudal segment showing the posterior spiracles and anus of *Acroceratitis ceratitina* (SEM micrographs). A – caudal segment. B – posterior spiracles. C – anal lobes. D – creeping welt of fifth abdominal segment. Abbreviations: an – anal lobe, cr – caudal ridges, es – ecdysial scar, pds – posteriorly directed spinules, sh – spiracular hair, ss – small spinules.

2C). Creeping welt as in abdominal segments II–VII but central band of very small spinules nearly absent.

Puparium. Brown, 5.3–6.2 mm long (median = 5.4 mm; n = 5), and 2.2–2.7 mm wide (median: 2.3 mm; n = 5). Thoracic segments strongly tapering towards anterior end; abdominal segments more parallel sided, broadest in the area of abdominal segments III and IV, slightly tapering towards posterior end.

Material examined. Thailand: Mae Hong Son, Pangmapha, between Soppong and Ban Nam Rin, larvae in cut, upright shoot of *Dendrocalamus* sp., 25.vi.2015, sample Z85/2/15(B), 5 specimens, leg. D. Kovac.

Distribution. India, China, Myanmar, and Thailand (Kovac et al., 2006).

Biology. Larvae were reared from small upright, already dead shoots of *Dendrocalamus strictus* (3×), *Dendrocalamus* sp. (3×), *Pseudoxytenanthera albociliata* (1×) and *Thyrsostachys siamensis* (1×; Fig. 3A). The shoots were up to 50 cm high. Larvae were found in June, August and September.

On two occasions larvae were also reared from freshly cut bamboo shoots of *Dendrocalamus* sp. bought at a Lahu sales booth in the Pangmapha district, two on 25 June and two on 30 June 2015. They were 30–40 cm long and enwrapped by overlapping internode sheaths. The shoots were transferred to a natural bamboo stand of *Dendrocalamus* sp. on the day of purchase; one shoot was laid on the ground and the other was placed in the upright position by digging its base into the ground (Fig. 3B).

On the same day females of *A. ceratitina* were seen to lay eggs under the sheaths, but only in upright shoots. Two weeks later only upright shoots contained *A. ceratitina* larvae, while shoots lying on the ground contained many larvae of the Gastrozonini *Gastrozona* spp. and *Chaetellipsis* spp.

Larvae of *A. ceratitina* fed inside the walls of the short, white and soft internodes. Some larvae also mined within the thickened base of the internode sheaths. There were more than 50 larvae per shoot (n = 5; two purchased shoots and three shoots found in the field). Younger larvae were yellow (Fig. 3C), older ones sometimes spotted yellow-orange and finally pale greenish (Fig. 3D). Mature larvae leaving the bamboo shoot readily skipped. First adults emerged 22 and 26 days after the purchased shoots were transferred to a bamboo stand.

Flies were recorded in the field between May and October. Females (Fig. 3E) were seen to oviposit below the protective culm sheaths of upright shoots of two undetermined *Dendrocalamus* species.

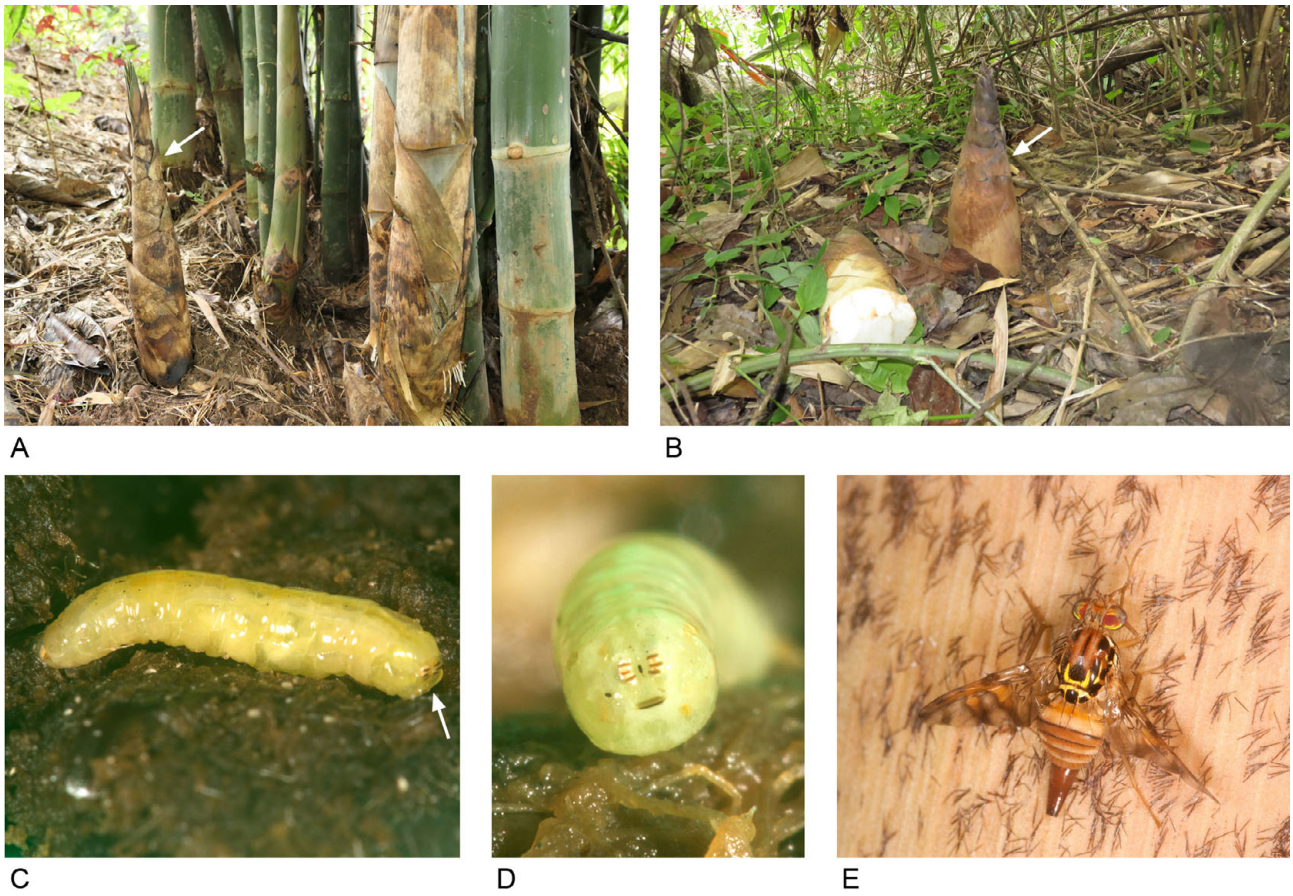

Fig. 3. Host plants, larva and female of *A. ceratitina*. A – dead upright shoot of *Thyrsostachys siamensis* (arrow). B – freshly cut bamboo shoots of *Dendrocalamus* sp. bought at a market and taken to the field where they were buried upright (arrow) into the ground or laid on their side. Only the upright shoot was infested by *A. ceratitina*. C – larva of *A. ceratitina*. Arrow points to the posterior spiracle. D – enlarged caudal part of *A. ceratitina*. E – female of *A. ceratitina* resting on a culm sheath of *Dendrocalamus strictus*.

Acroceratitis distincta (Zia, 1964)

Chelyophora distincta Zia, 1964.
Phaeospilodes fritilla Hardy, 1973.
Phaeospilodes distincta Wang, 1998.

Description

As in *A. ceratitina*, except:

Habitus. Length: 5.6–7.4 mm (median: 6.8 mm; n = 7); maximum width: 1.1–1.3 mm (median: 1.2 mm; n = 7). Mature larvae broadest in the area of abdominal segments IV–V.

Pseudocephalon (Fig. 4). Number of serrated oral ridges 13–14. With 12–14 serrated accessory plates.

Cephalic lobes moderately developed (Fig. 4A). Basal segment of antenna approximately cylindrical, apical segment cylindrical with rounded tip. Maxillary palpus surrounded by a complete cuticular fold (Fig. 4C).

Primary preoral lobe rounded; number of preoral lobes 11–13 (Fig. 4D). Preoral organ bearing three peg, one papillar, and two pit sensilla. Basal surface of labial lobe covered with well-developed tubercles (Fig. 4E). Papillar sensilla close to labial organ lacking.

Cephalopharyngeal skeleton (Fig. 16). Total length 0.8–0.9 mm (median: 0.82 mm; n = 6). Indentation between apex of apical tooth and ventral apodeme 0.15–0.18× as deep as mouthhook length; apical tooth brown, neck well developed; preapical tooth about 0.005 mm long. Ventral apodeme triangular shaped. Hypopharyngeal sclerite 2.6–3.4× as long as high. Hypopharyngeal bridge, brown, 0.01–0.02 mm long, about 0.02 mm wide, located between the anterior four sevenths and the posterior three sevenths of the length of the hypopharyngeal sclerite. Dorsal and ventral cornua brown, hyaline areas at posterior tip and ventral margin of ventral cornu; brown area of dorsal cornu slightly shorter than brown area of ventral cornu. Parastomal bars of approximately the same length as hypopharyngeal sclerite, in two specimens hooked at apex (in one of these two specimens only one parastomal bar hooked at apex). Anterior sclerite lacking in four of six examined specimens.

Thorax. Anterior spiracles with 13–14 tubules (Fig. 4F). Anterior margins of second and third thoracic segment with 4–6 rows of stout spinules.

Abdominal segments I–VII. First abdominal creeping welt bearing a band of very small spinules anteriorly and about 7 rows of posteriorly directed spinules posteriorly; creeping welts of abdominal segments II–VII bearing rows of spinules arranged as follows (from anterior to posterior): 5–6 rows of anteriorly directed spinules, a band of very small spinules, being very narrow (about one row) in the middle, 4–7 rows of stout posteriorly directed spinules, a

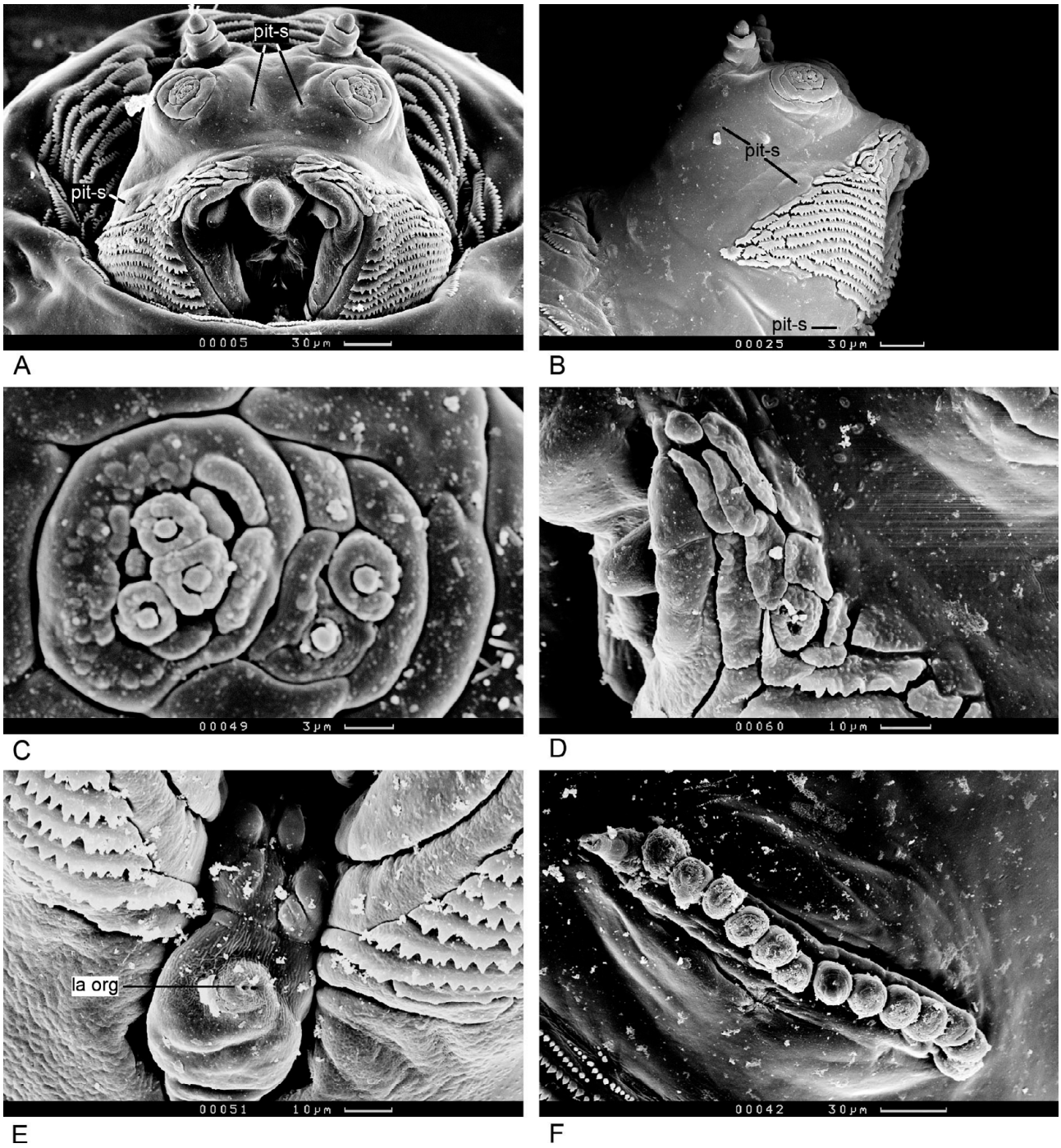

Fig. 4. Pseudocephalon and anterior spiracle of *Acroceratitis distincta* (SEM micrographs). A – pseudocephalon, frontal view. B – pseudocephalon, lateral view. C – maxillary sense organ. D – preoral organ located on primary preoral lobe, surrounded by remaining preoral lobes. E – labial lobe. F – anterior spiracle. Abbreviations: la org – labial organ, pit-s – pit sensillum.

band of very small spinules, 4–5 rows of large posteriorly directed spinules (Fig. 5D). Bands of very small spinules of the creeping welts also covering anterior margins of abdominal segments ventrolaterally.

Caudal segment (Figs 5A–C and 16). Shortest distance between spiracles 0.5–0.8× as long as longest spiracular opening. Angle between dorsal and central opening up to 25°, shortest distance between dorsal and central opening somewhat more than half as long as longest opening; angle between central and ventral opening 1–29°, shortest distance between central and ventral opening one third to half as long as longest opening. Spiracular openings 4.0–6.0× as long as wide. Spiracular hairs up to half as long as longest spiracular opening, hairs branched up to 5×; dorsal bundle containing 5–12 hairs, ventral bundle containing 5–10 hairs, dorsolateral bundle containing 2–4 hairs, ventrolateral bundle containing 4–7 hairs (Figs 16 and 5B).

Anal lobes surrounded by 3–5 rows of large, pointed spinules and anterolaterally by an additional patch of very small spinules (Fig. 5C). Creeping welt bearing rows of spinules arranged as follows (from anterior to posterior): A band of very small spinules, about 5 rows of stout posteri-

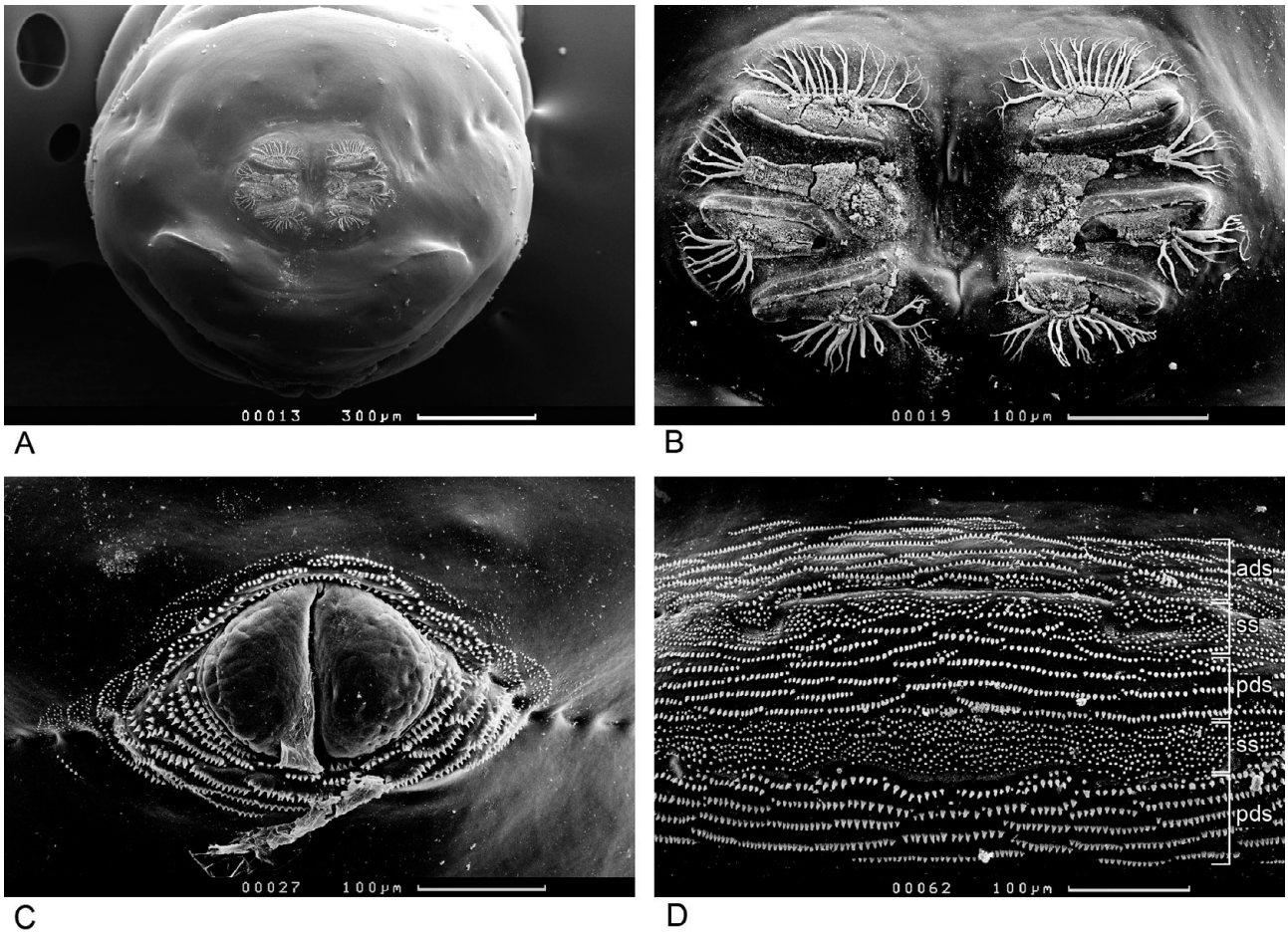

Fig. 5. Creeping welt and caudal segment showing the posterior spiracles and anus of *Acroceratitis distincta* (SEM micrographs). A – caudal segment. B – posterior spiracle. C – anal lobes. D – creeping welt of fifth abdominal segment. Abbreviations: ads – anteriorly directed spinules, pds – posteriorly directed spinules, ss – small spinules.

orly directed spinules, a band of very small spinules, about 4 rows of stout posteriorly directed spinules.

Puparium. Puparia brown, 3.4–4.2 mm long (median: 4.0 mm; n = 5), and 1.5–1.8 mm wide (median: 1.8 mm; n = 5). Thoracic segments strongly tapering toward anterior end; abdominal segments more parallel sided, broadest in the area of the third abdominal segment, slightly tapering toward posterior end.

Material examined. Thailand: Mae Hong Son, Pangmapha, between Soppong and Ban Nam Rin, larvae in shoots of *Dendrocalamus* sp. and *D. strictus*, 15.vi.2015, sample Z61/1/15, 8 specimens and 15.vi.2015, sample Z64/1/15, 2 specimens, all leg. D. Kovac.

Distribution. India, China, Laos, Thailand, and Vietnam (Kovac et al., 2006).

Biology. In previous studies *A. distincta* was reared from *Bambusa pallida*, *B. tulda*, *B. vulgaris*, *B.* sp., *Dendrocalamus asper*, *D. strictus, Thyrsostachys siamensis*, *Pseudoxytenanthera albociliata* (*Melocalamus compactiflorus* in Dohm et al., 2014) and *Cephalostachyum pergracile* (Allwood et al., 1999, Dohm et al., 2014). Biological details were not known. In the present study *A. distincta* larvae were found between July and November and reared from bamboo shoots of *Pseudoxytenanthera albociliata* (14×), *Cephalostachyum pergracile* (5×), *Dendrocalamus strictus* (5×), *Dendrocalamus* sp. (1×) and *Bambusa polymorpha* (1×). Larvae infested exclusively thin stems of living or freshly cut bamboo shoots placed in the upright position or lying on the ground.

In the smaller bamboo species *P. albociliata* larvae infested 1–3 internodes located next to each other (Fig. 6A), usually the 3rd–5th internode below shoot apex. The base of the lowest infested internode was located 16–45 cm below shoot apex (n = 4). Infested internodes and apex of the shoot died off and could be easily recognized by the withered sheath blades (Fig. 6A). After a while apical internodes would fall to the ground, whereas the lowest infested internode remained attached to the shoot for a longer time (Fig. 6B). Buds located at the base of the lowest infested internode remained intact.

In larger bamboo species, i.e., *C. pergracile*, *D. strictus* and *D.* sp., larvae of *A. distincta* only infested thin shoots, which mostly grew in young bamboo stands. Mid-sized to large shoots (diameter about 4 cm or larger) were not colonized, but larvae were found in side branches of large *D. strictus* shoots (Fig. 6C).

Larvae of *A. distincta* fed in the basal 1/3–2/3 of the infested internodes. In advanced stage of larval development the feeding area consisted of three clearly distinguishable zones. The basal part of the internode wall was entirely

Fig. 6. Host plant, larvae and female of *A. distincta*. A – shoot of *Pseudoxytenanthera albociliata* infested by *A. distincta* larvae. The apical part of the shoot has died off due to the larval feeding activity and the leaf-like sheath blades have withered. The arrows point to the two internodes infested by *A. distincta* larvae. The lower infested internode was 12.2 mm in diameter. B – *Pseudoxytenanthera albociliata* internode infested by *A. distincta*. The internode has turned brown, whereas the sheath is still green. The apical part of the shoot has fallen to the ground. C – location of infested internodes in two side branches of *A. strictus* (arrows). D – larva of *A. distincta* boring in a thin stem of a *P. albociliata* shoot, which was cut off and placed on the ground. E – larva of *A. distincta* feeding in the pulpy basal area of an internode. F – larvae of *A. distincta* feeding in the fibrous apical area of an internode. G – female ovipositing below the sheath edge of a cut shoot of *P. albociliata* lying on the ground.

eaten up over a length of up to 6 cm. The adjacent area consisted of small bamboo particles and was of pulpy consistency or turned crumbly after desiccation (Fig. 6E). The upper feeding area was characterized by fibrous vascular bundles, since the larvae apparently fed on the parenchyma cells in which the vascular bundles were embedded (Fig. 6F). Usually, larvae did not enter the internode cavity. Although the basal part of the infested internode wall was

totally devoured, the upper part remained attached to the shoot, because it was firmly held in place by the enveloping sheath.

Infested internodes belonging to different bamboo species were 5.5–32 cm long (median = 19.4 cm, n = 14) and 4–28 mm wide (median = 12 mm, n = 15). They usually contained 10–20 larvae per internode, depending on internode size. For example, a small internode measuring 6 cm × 4 mm contained 9 larvae and a larger internode measuring 25 cm × 12 mm contained 22 larvae. The number of larvae found in some internodes was low despite the large proportion of eaten bamboo tissue, suggesting that some larvae had already left the internode. Mature larvae (Fig. 6D–F) were dark yellow and readily skipped when disturbed. In four larvae from different shoots the duration between oviposition and emergence of first adults amounted to 25, 27, 30 and 35 days. In the field larvae left their internode for pupariation in the soil. In the rearing boxes most larvae pupariated between moistened tissue, however, some puparia were also found between fibers inside the internodes.

Larvae developing in side branches of *D. strictus* shoots were found near the branch apex (Fig. 6C). The infested internodes died off, changed color from green to brown and became soft. After the larvae had left, the apical part of the side branch including the infested internode fell to the ground, whereas the remaining part of the side branch remained intact.

Flies were common in the study area and were collected during all months between March and December. In the lab, some flies emerged in January and one fly on 2nd February. Females laid eggs by inserting their aculeus below the edge of the internode sheath, usually near the base of the internode (Fig. 6G). In one case a female was observed inserting her ovipositor below a sheath of a larger shoot of *Dendrocalamus* sp. beside an ovipositing *A. incompleta*. Flies dabbed on items containing sweat (cloth of sweeping net, surface of backpack, knife handle, walking stick) and on leaves covered with urine. Altogether, 80 males and 5 females were collected from the sweeping net or backpack lying on the ground and 23 males and 1 female from leaves covered with urine on various dates between 2007 and 2017. On one occasion, 27 September 2017, *A. distincta* was collected from fresh sweat and urine for 1.5 h. The collecting yielded 14 males and 4 females on net/ backpack and 19 males and 1 female on urine.

Acroceratitis histrionica (Meijere, 1914)

Chelyophora histrionica Meijere, 1914.

Description

As in *A. distincta* except:

Habitus. Length: 6.8–9.2 mm (median: 7.8 mm; n = 5); maximum width: 1.1–1.4 mm (median: 1.2 mm; n = 5). Mature larvae broadest in the area of abdominal segments III–V.

Pseudocephalon (Fig. 7). Number of irregularly serrated oral ridges 7–9. With 8–10 accessory plates.

Number of preoral lobes 9–10 (Fig. 7D). Preoral organ bearing two to three peg, one papillar, and one pit sensilla.

Cephalopharyngeal skeleton (Fig. 16). Total length 0.9–1.1 mm (median: 1.0 mm; n = 5). Indentation between apex of apical tooth of mouthhooks and ventral apodeme 0.13–0.21× as deep as mouthhook length; apical tooth dark brown, strongly curved; preapical tooth 0.011–0.016 mm long. Hypopharyngeal sclerite 3.6–5.1× as long as high. Hypopharyngeal bridge about 0.02 mm long and wide, located somewhat posterior to middle of hypopharyngeal sclerite. Dorsal and ventral cornua light brown; hyaline areas at posterior tips of both cornua and ventral margin of ventral cornu; light brown areas of both cornua of virtually the same length. Parastomal bars about 0.9× as long as hypopharyngeal sclerite, in two observed specimens with hooked apex. Anterior sclerite light brown, present only in two of five examined specimens.

Thorax. Anterior spiracles with 15–16 tubules (Fig. 7F).

Abdominal segments I–VII. First abdominal creeping welt bearing about 3 rows of anteriorly directed spinules anteriorly and about 8 rows of posteriorly directed spinules posteriorly; laterally slender, wedge-shaped areas covered with very small spinules inserted in creeping welt; creeping welts of abdominal segments II–VII bearing rows of spinules arranged as follows (from anterior to posterior): 5–7 rows of anteriorly directed spinules, 7–10 rows of posteriorly directed spinules, 3–4 rows of curved anteriorly directed spinules, 4–6 rows of long posteriorly directed spinules; laterally wedge-shaped areas covered with very small spinules inserted in creeping welts (Fig. 8D–F). Anterior margin of first abdominal segment lined with about 5 rows of posteriorly directed spinules, laterally a band of very small spinules located anteriorly to these spinules. Anterior margins of second to fifth abdominal segments lined with a band of very small spinules anteriorly and few irregular rows of posteriorly directed spinules posteriorly. Anterior margin of sixth abdominal segment bearing very small spinules laterally.

Caudal segment (Figs 16 and 8A–C). Shortest distance between spiracles 0.6–0.9× length of longest spiracular opening. Angle between dorsal and central opening up to 12°, shortest distance between dorsal and central opening somewhat more than half as long as longest opening; angle between central and ventral opening 24–33°, shortest distance between central and ventral opening one fourth to one third as long as the longest opening. Spiracular openings 5.4–7.3× as long as wide. Spiracular hairs up to 0.6× as long as longest spiracular opening; dorsal bundle containing 2–12 hairs, ventral bundle containing 5–9 hairs, dorsolateral bundle with 3–5 hairs, ventrolateral bundle with 2–7 hairs (Figs 16 and 8B).

Dark transverse line on caudal area usually present. Anal lobes surrounded by 3–4 rows of pointed spinules. A group of small spinules located lateral to anal lobes (Fig. 8C). Creeping welt as in abdominal segments II–VII.

Puparium. Puparia brown, 3.6–4.1 mm long (n = 2) and 1.7–1.8 mm wide (n = 2). Thoracic segments strongly tapering towards the anterior end; abdominal segments more

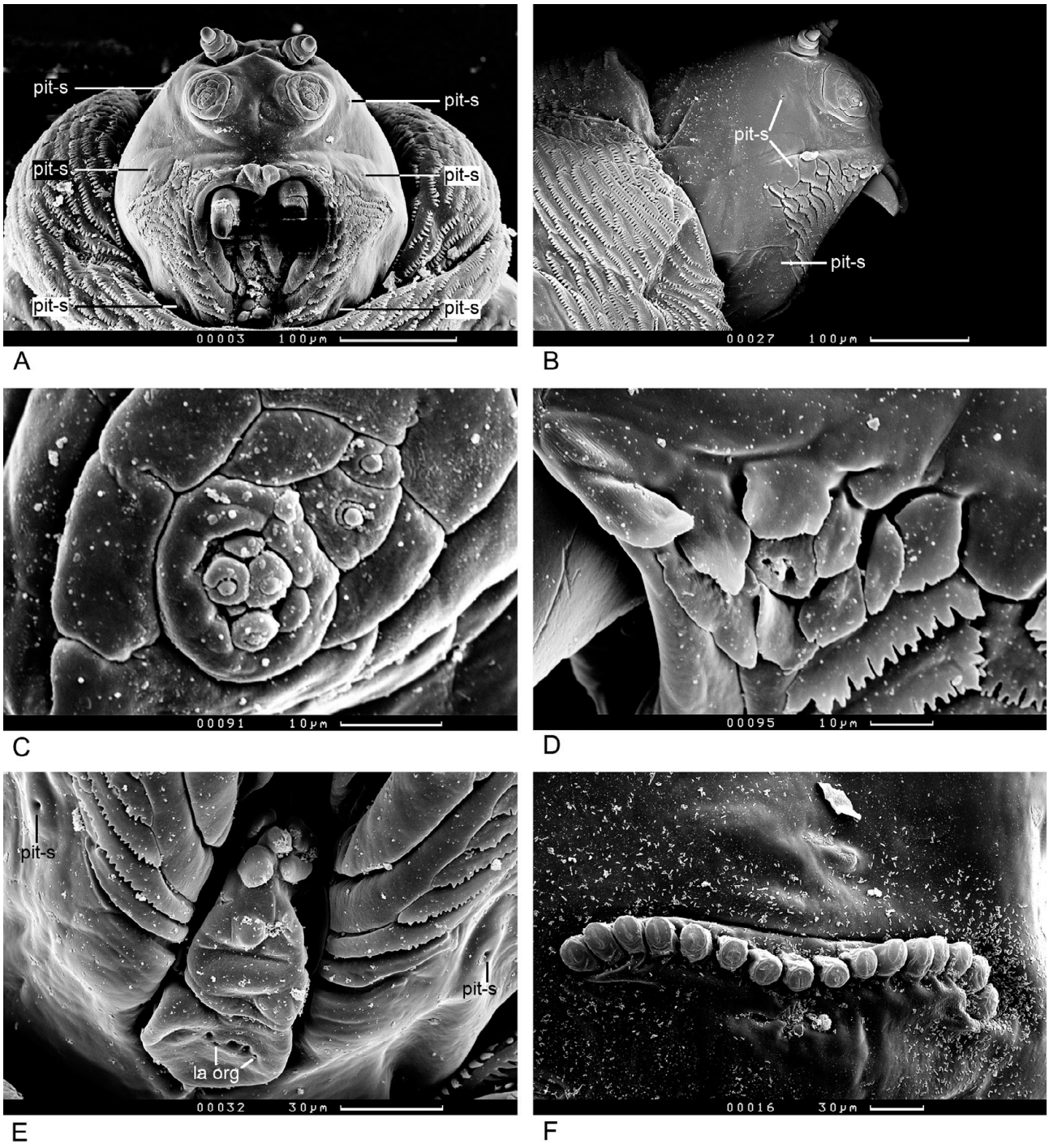

Fig. 7. Pseudocephalon and anterior spiracle of *Acroceratitis histrionica* (SEM micrographs). A – pseudocephalon, frontal view. B – pseudocephalon and part of the first thoracic segment, lateral view. C – maxillary sense organ. D – preoral organ located on primary preoral lobe, surrounded by remaining preoral lobes. E – labial lobe. F – anterior spiracle. Abbreviations: la org – labial organ, pit-s – pit sensillum.

parallel sided, broadest at the third abdominal segment, slightly tapering towards the posterior end.

Egg. Length: 1.5 mm, width: 0.3 mm; elongate, asymmetrical, one side nearly straight, the other side somewhat rounded, anterior and posterior end similarly rounded, anterior end with small pedicel. Pedicel wider than long (0.06: 0.03 mm), somewhat truncate anteriorly; no aeropyles visible. Surface of egg shell entirely covered by net-like sculpture.

Empty shells of eggs: As described for egg except: Length: 1.5–1.8 mm (median: 1.7 mm; n = 10), width: 0.3–0.4 mm (median: 0.35 mm; n = 10); elongate, tapering towards the posterior end over about half of its length, anterior end rounded, with small pedicel. Pedicel wider (0.05–0.07 mm; median: 0.06 mm; n = 10) than long (0.02–0.04 mm; median: 0.03 mm; n = 10).

Material examined. Thailand: Mae Hong Son, Pangmapha, between Soppong and Ban Nam Rin, larvae in shoots of *Dendro-*

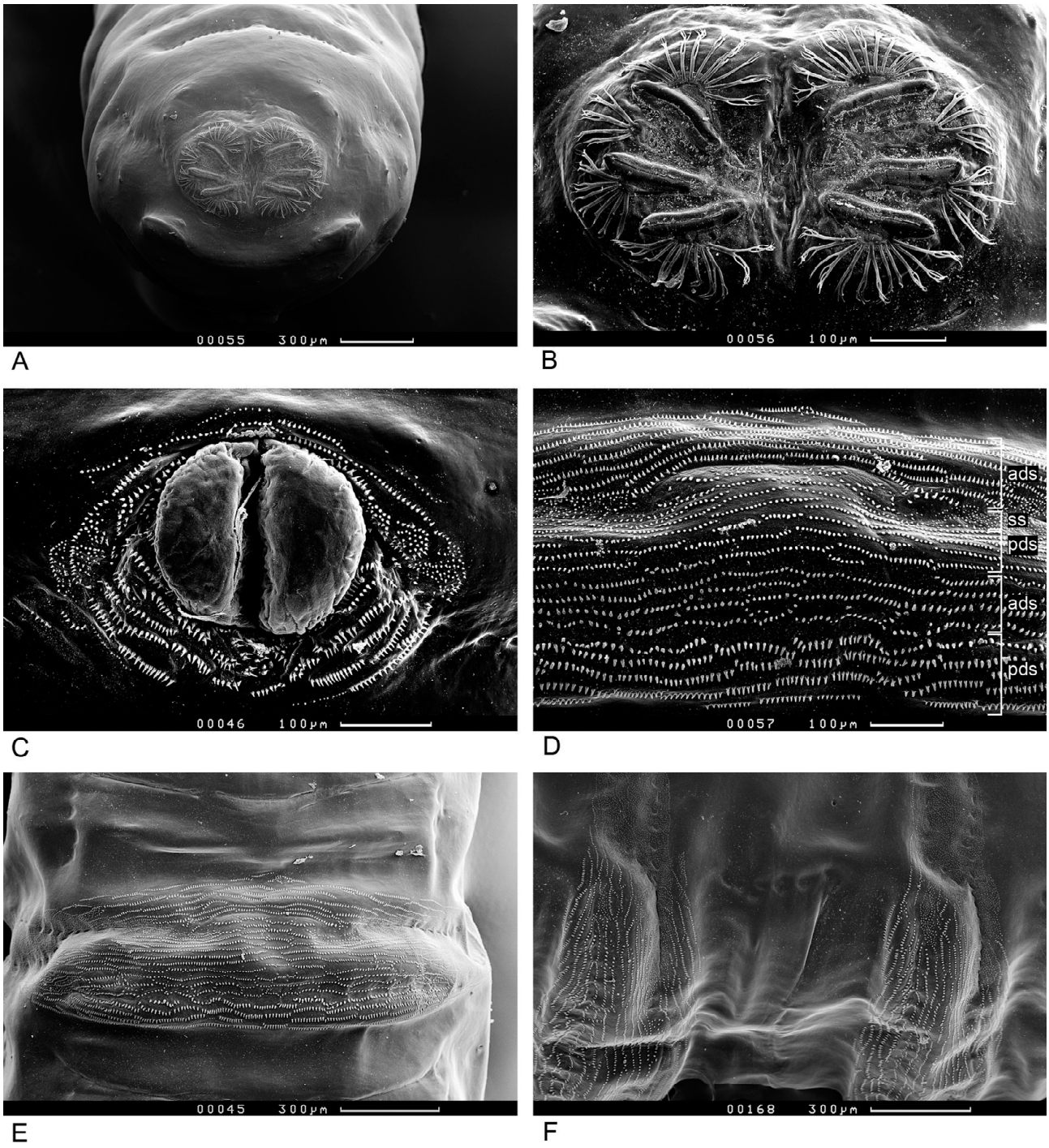

Fig. 8. Creeping welt and caudal segment showing the posterior spiracles and anus of *Acroceratitis histrionica* (SEM micrographs). A – caudal segment. B – posterior spiracle. C – anal lobe. D – creeping welt of fifth abdominal segment. E – overview of creeping welt of fourth abdominal segment. F – ventrolateral view of creeping welts of third (right) and fourth (left) abdominal segments. Abbreviations: ads – anteriorly directed spinules, pds – posteriorly directed spinules, ss – small spinules.

calamus strictus, 18.ix.2010, sample T20/2010b, 5 specimens and 21.vi.2015, sample Z79/1/15, 3 specimens, all leg. Kovac.

Distribution. China, Sri Lanka, Thailand, Laos, Malaysia, and Indonesia (Kovac et al., 2006, Yu et al., 2010).

Biology. So far, *A. histrionica* larvae were reared from *Gigantochloa albociliata* and *Dendrocalamus strictus* (Allwood et al., 1999; Dohm et al., 2014). In the present study larvae were reared from living shoots of *Dendrocalamus strictus* (6×), *D. hamiltoni* (1×) and *D.* sp. (1×). Larvae were found in the field between June and beginning of December.

Based on observations of D. Kovac (in Dohm et al., 2014 and unpubl. observ.), *A. histrionica* larvae developed on the surface of mid-sized to large bamboo shoot stems below the protective culm sheaths (internode diameters 1.2 to 11 cm; Fig. 9A). The larval feeding site was always located in the area above the branch bud, which was situated at the base of the internode. The alternately arranged

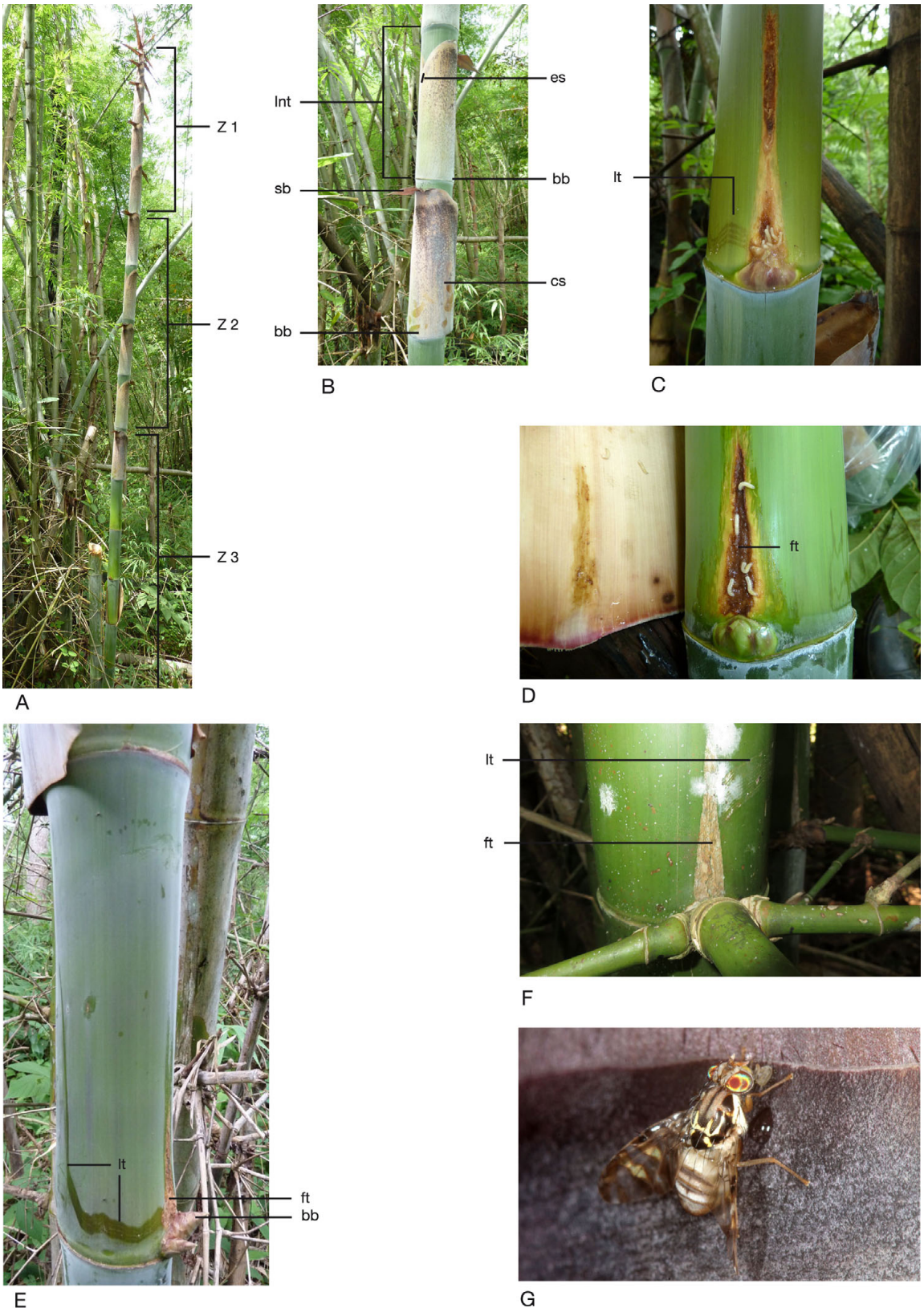

Fig. 9. Host plant, larvae and female of *Acroceratitis histrionica*. A – shoot of *Dendrocalamus strictus*. In the upper zone (Z1) the shoot is covered by several layers of culm sheaths; in the central zone (Z2) the culm sheaths are shorter than the internodes and protect the softer, lower parts of the internodes; and in the basal zone (Z3) sheaths get loose and then fall to the ground. B – detail of bamboo shoot internodes of *D. strictus* showing the location of the branch buds and the egg-laying site. C and D – *A. histrionica* larvae feeding in a triangular area ("feeding triangle") above the branch bud (sheaths removed). E – larval tracks showing the path from the egg-laying to the feeding site. The larvae have already left their feeding site and the sheath has fallen down. F – internode of a mature bamboo culm showing old larval tracks and feeding marks of *A. histrionica*. G – male of *A. histrionica*. Abbreviations: bb – branch bud, cs – culm sheath, es – egg-laying site, ft – feeding triangle, Int – internode, lt – larval tracks, sb – sheath blade.

branch buds were located on the opposite side of the area where the internode sheath was overlapping (Fig. 9B). In *D. strictus* branch buds occurred on all culm internodes, and *A. histrionica* larvae were found all along the shoot stem (base of lowermost colonized internode located 30 cm above ground; n = 8), while in *D. hamiltoni* and *D.* sp. branch buds formed from mid-culm upwards (base of lowermost colonized internode 3.22 m above ground; n = 3).

Eggs hatched below the upper edge of the sheath, and larvae squeezed their way down between the bamboo surface and the sheath towards their feeding site at the base of the internode. Sometimes, freshly hatched larvae left a permanent track on the bamboo surface enabling the reconstruction of the larval path towards their feeding site (Fig. 9C, E, F). Judging from the tracks the larvae squeezed diagonally downwards, probably along the concealed sheath edge covered by the opposite end of the sheath. The beginning portion of the path was narrow, indicating that initially the larvae followed each other. Further down at the level of the prospective "feeding triangle" (see below) the path became wider and then split into several roughly horizontal, parallel branches, indicating that the larvae independently changed their directions towards their feeding site. The larvae reached their feeding site somewhere between the base and the tip of the prospective "feeding triangle". In several cases indentations leading to the feeding triangle were visible, but feeding marks were lacking.

Young *A. histrionica* larvae scraped bamboo tissue from the bamboo shoot, thus leaving small, pale feeding marks on the green internode surface (Fig. 9C). At a later stage of larval development the feeding area became larger and the vascular fibers became visible. The final shape of the brownish feeding area resembled an upward pointing triangle with the base being located at the level of the branch bud and its tip sometimes reaching up to the center of the internode (Fig. 9D). The larvae exploited only the softer substrate of the bamboo surface or substrate between the vascular fibers and did not penetrate into the already hardened internode wall. They also did not damage the branch buds, which were protected by their own small sheaths (prophylls). The feeding area above the branch bud was moist. Sometimes, water filled the space between the bamboo surface and the sheath and larvae appeared to be dead, but they often started to move after a few minutes. There were 3–13 larvae per internode (median = 6, n = 31). Young larvae were pale, while mature larvae turned yellow at the very end of their development. Mature larvae readily skipped when disturbed.

Large shoots of *D. strictus* and other bamboo species could be divided into three vertical zones regarding the developmental stage of their internodes and the degree of the protection by the culm sheaths (Fig. 9A): In the apical zone (Z1) the newly developing internodes were short and soft. The respective sheaths were much longer than the internodes and covered the shoot surface in several overlapping layers. In the central zone (Z2) the internodes were elongated and their already hardened apical parts were sticking out from their sheaths. Thus, the sheaths enclosed mainly the lower, softer parts of the internodes. In the basal zone (Z3) the bases of the internodes were still more hardened and the protective sheaths gradually loosened and fell off to the ground.

The vertical succession of the internode development was reflected by the vertical succession of larval developmental stages of *A. histrionica*. At the base of the apical shoot zone Z1 eggs and freshly hatched larvae were found. In the central zone Z2 the upper internodes contained small larvae with inconspicuous feeding marks (feeding area still green), while in the lower part of zone Z2 the internodes contained larger larvae with a conspicuous large brownish feeding area. In the basal zone Z3 the sheaths of the upper internodes were loosened and just a small number of mature larvae were present, indicating that some had already left the internode for pupariation. In the lower internodes of zone Z3 both sheaths and larvae were lacking, but feeding marks indicated that *A. histrionica* had been present.

Acroceratitis histrionica flies (Fig. 9G) were recorded between March and October. Females oviposited below culm sheaths, about 1–6 mm from the sheath edge. Eggs were laid in clusters of several eggs. In one case eggs were found in five sheaths lying adjacent to each other at a height between ca. 1.50 m and 1.80 m (height of shoot ca. 2.50 m). There were 8; 10; 13; 16 and 20 eggs per sheath. The oviposition site was situated in the area where the culm sheath was overlapping, ca. 8–9 cm below the upper margin of the sheath (Fig. 9B).

Acroceratitis incompleta Hardy, 1973

Description

As in *A. ceratitina*, except:

Habitus. Length: 9.1–9.9 mm (median: 9.3 mm; n = 5); maximum width: 1.4–1.7 mm (median: 1.6 mm; n = 5). Mature larvae broadest in the area of abdominal segments IV–VIII.

Pseudocephalon (Fig. 10). Number of oral ridges 14–16. With 13–17 serrated accessory plates.

Cephalic lobes moderately developed (Fig. 10A). Apical segment of antenna cylindrical with rounded tip. Maxillary palpus surrounded by a complete cuticular fold (Fig. 10C).

Primary preoral lobe rounded; number of preoral lobes 9–12 (Fig. 10D). Preoral organ bearing three peg, one papillar, and one pit sensilla. Surface of labial lobe entirely smooth.

Cephalopharyngeal skeleton (Fig. 16). Total length 1.0–1.1 mm (median: 1.0 mm; n = 6). Indentation between apex of apical tooth of mouthhooks and ventral apodeme 0.17–0.23× as deep as mouthhook length; neck well developed; preapical tooth 0.005–0.010 mm long; ventral apodeme posteroventrally directed. Hypopharyngeal sclerite 3.6–4.4× as long as high. Hypopharyngeal bridge about 0.02 mm long, 0.02–0.03 mm wide, located slightly posterior of middle of hypopharyngeal sclerite. Hyaline areas at posterior tips of both cornua and at ventral margin of ventral cornu; brown areas of both cornua of virtually the same length. Anterior sclerite present in four of six examined specimens.

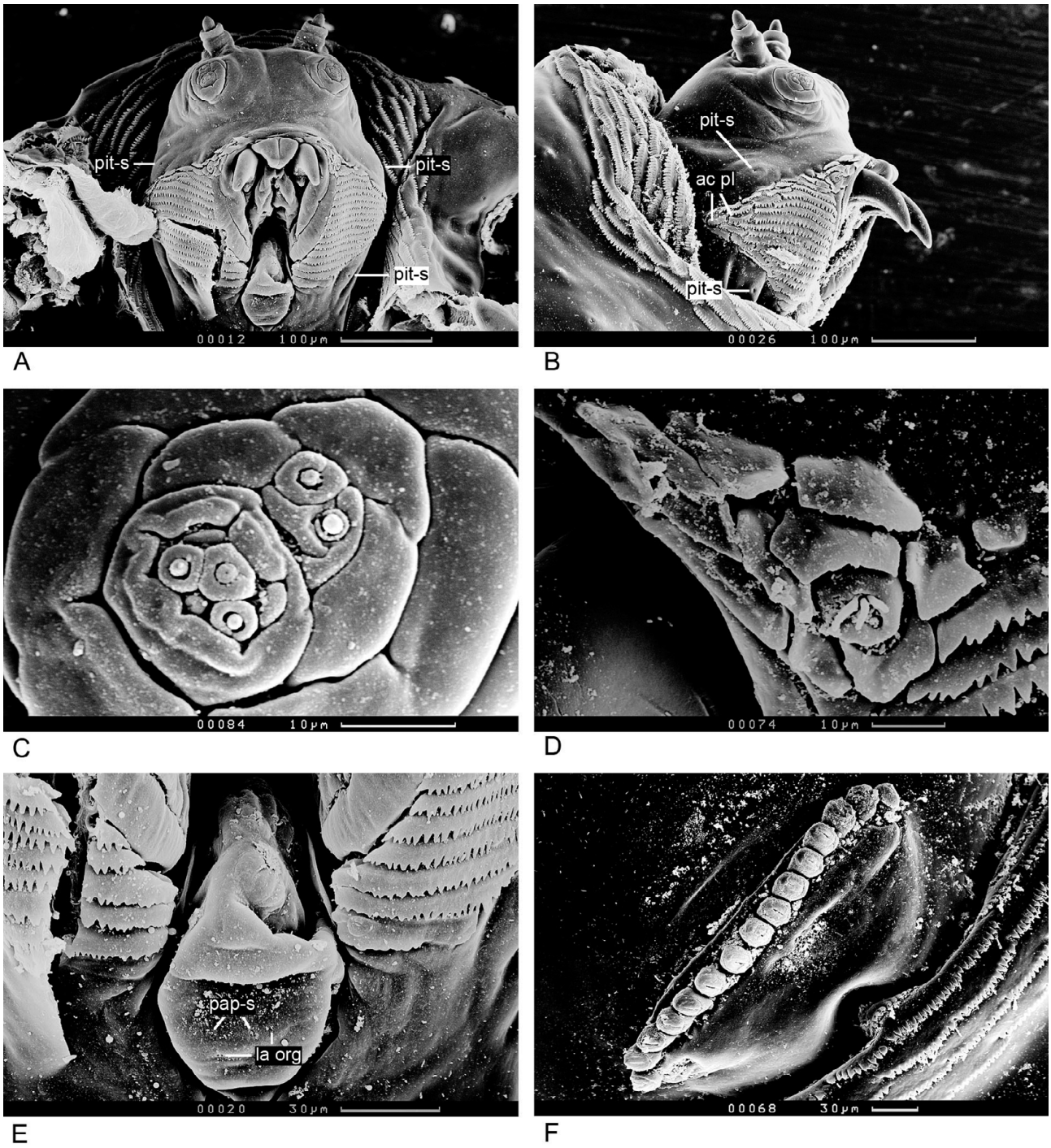

Fig. 10. Pseudocephalon and anterior spiracle of *Acroceratitis incompleta* (SEM micrographs). A – pseudocephalon, frontal view. B – pseudocephalon and part of the first thoracic segment, lateral view. C – maxillary sense organ. D – preoral organ located on primary preoral lobe, surrounded by remaining preoral lobes. E – labial lobe. F – anterior spiracle. Abbreviations: la org – labial organ, pap-s – papillar sensillum, pit-s – pit sensillum.

Thorax. Anterior spiracles with 15–16 tubules (Fig. 10F). Anterior margin of second thoracic segment with about 5 rows of spinules dorsolaterally and about 2 rows expanding from the ventral to the lateral side, a narrow area without spinules dorsally. Anterior margin of third thoracic segment with about 3 rows of spinules dorsolaterally and about 2 rows expanding from the ventral to the lateral side, an area without spinules dorsally.

Abdominal segments I–VII. First abdominal creeping welt bearing a band of very small spinules, arranged in patches anteriorly and about 8 rows of posteriorly directed spinules posteriorly; creeping welts of abdominal segments II–VII bearing rows of spinules arranged as follows (from anterior to posterior): A band of very small spinules, arranged in patches, 7–9 rows of posteriorly directed spinules, a band of very small spinules, 4–5 rows of poste-

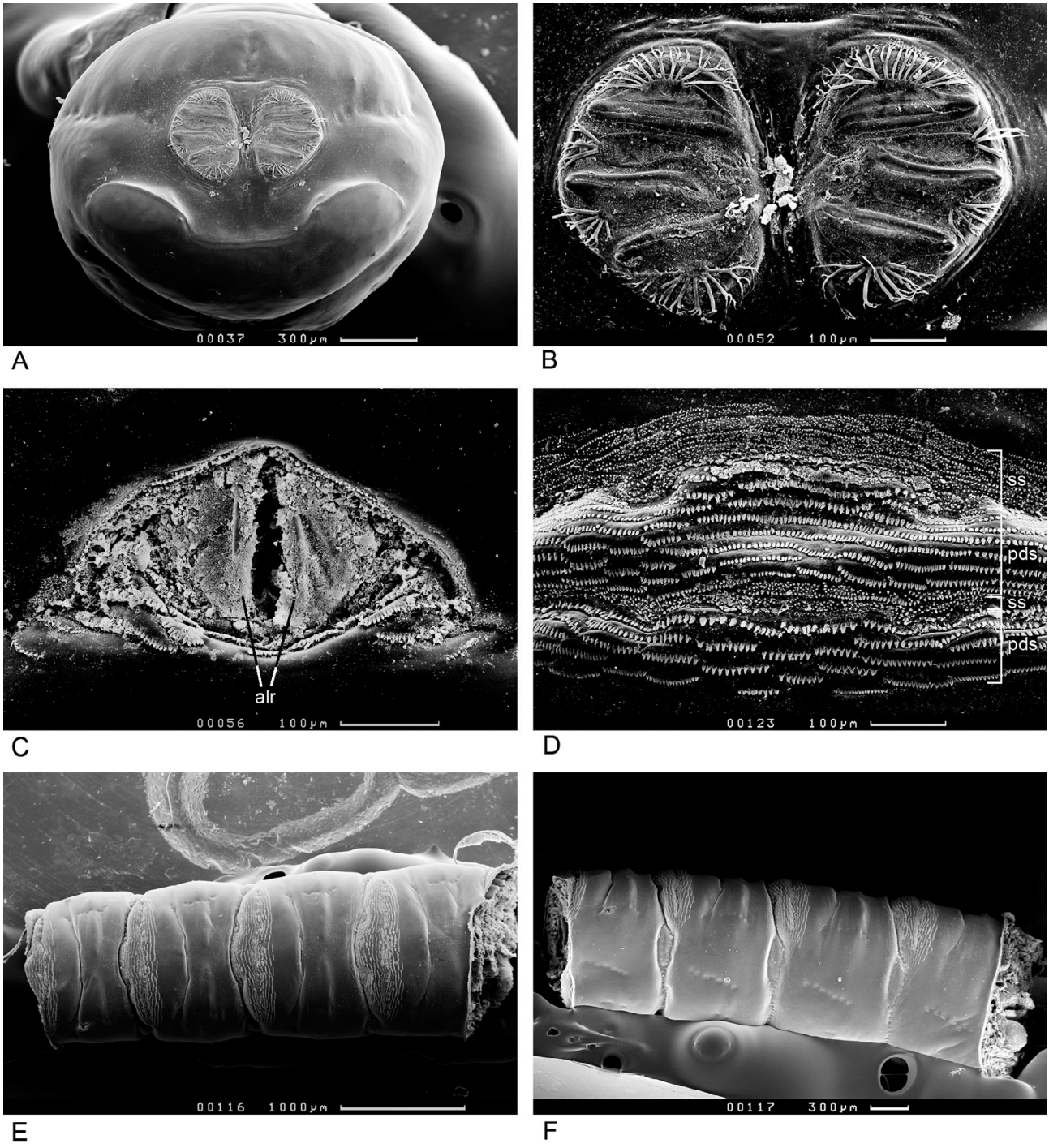

Fig. 11. Abdomen, creeping welts and caudal segment showing the posterior spiracles and anus of *Acroceratitis incompleta* (SEM micrographs). A – caudal segment. B – posterior spiracles. C – anal lobes. D – creeping welt of seventh abdominal segment. E – abdominal segments 2–5 in ventral view. F – abdominal segments 2–5 in lateral view. Abbreviations: alr – anal lobe ridges, pds – posteriorly directed spinules, ss – small sensilla.

riorly directed spinules (Fig. 11D–F). Anterior margin of first abdominal segment with posteriorly directed spinules laterally. Anterior margins of remaining abdominal segments laterally with bands of very small spinules.

Caudal segment (Figs 16 and 11A–C). Shortest distance between spiracles about 0.4× as long as longest spiracular opening. Angle between dorsal and central opening up to 12°, shortest distance between dorsal and central opening about one fourth to one third as long as longest opening; angle between central and ventral opening 7–23°, shortest distance between central and ventral opening about 0.1–0.2× as long as longest opening. Spiracular openings 6.7–9.4× as long as wide. Spiracular hairs up to half as long as longest opening; dorsal bundle containing 8–15 hairs, ventral bundle containing 7–14 hairs, dorsolateral bundle containing 2–4 hairs, ventrolateral bundle containing 3–7 hairs (Figs 16 and 11B).

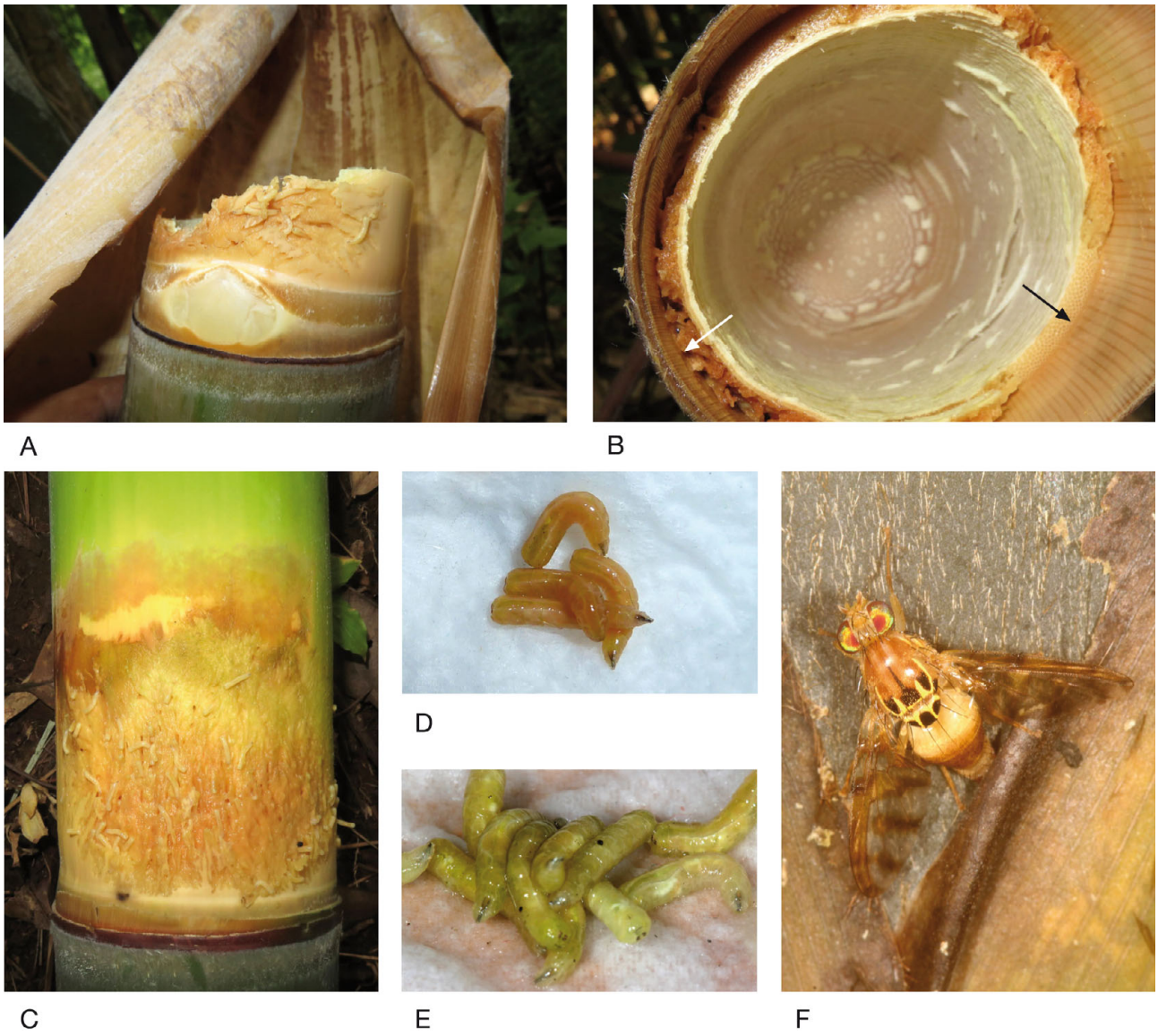

Fig. 12. Host plant, larvae and female of *A. incompleta*. A – young larvae of *A. incompleta* feeding on the shoot surface in the basal part of an internode. The upper part of the internode and the sheath were removed. B – apical part of an infested internode seen from below. One side of the wall was largely eaten up (left, white arrow), while the other side is intact and solid (right, black arrow). The larvae did not pierce the pith ring nor enter the internode cavity. C, D and E – body color changes during larval development from milky-pale to yellow (C) and then to yellow-orange (D) and yellow-green (E). F – *Acroceratitis incompleta* female laying eggs below the sheath edge of a *D. strictus* shoot.

Anal lobes slightly protuberant, with longitudinal ridge (elongate elevation of the surface of the anal lobe, bordering the opening of the anus; Fig. 11C) on each lobe. Few rows of anteriorly directed spinules anterior to anal lobes and rows of dentate scales posterior to anal lobes (Fig. 11C). Creeping welt as in abdominal segments II–VII.

Puparium. Brown, 5.1–6.0 mm long (median: 5.7 mm; n = 5) and 2.3–2.4 mm wide (median: 2.3 mm; n = 5). Thoracic segments strongly tapering towards anterior end; abdominal segments more parallel sided, broadest at the third abdominal segment, slightly tapering towards the posterior end.

Material examined. Thailand: Mae Hong Son, Pangmapha, near Ban Nam Rin in cut shoots of *Pseudoxytenanthera albociliata* lying on the ground, 17.x.2010, sample Z48/2/2010b, 2 specimens; near Ban Nam Rin, larvae in cut, upright shoots of *Dendrocalamus* sp., 19.x.2015, sample Z7/1/2015b, 6 specimens, all leg. D. Kovac.

Distribution. China, Thailand, and Laos (Kovac et al., 2006).

Biology. According to Dohm et al. (2014), *A. incompleta* larvae were reared from *Bambusa polymorpha, Dendrocalamus* sp. and *Melocalamus compactiflorus* (= *Pseudoxytenanthera albociliata*). In the present study *A. incompleta* was reared in October from *Dendrocalamus strictus* (cut upright shoot, 1×), *Dendrocalamus* sp. (cut upright shoot, 5×), *Bambusa polymorpha* (cut shoot lying on the ground, 1×) and *Pseudoxytenanthera albociliata* (cut shoot lying on the ground, 1×).

Young larvae fed on white, soft substrate of internodes located about 80 cm below the shoot apex (basal third of the Z1 area, see Fig. 9A). The larvae occupied 1–2 inter-

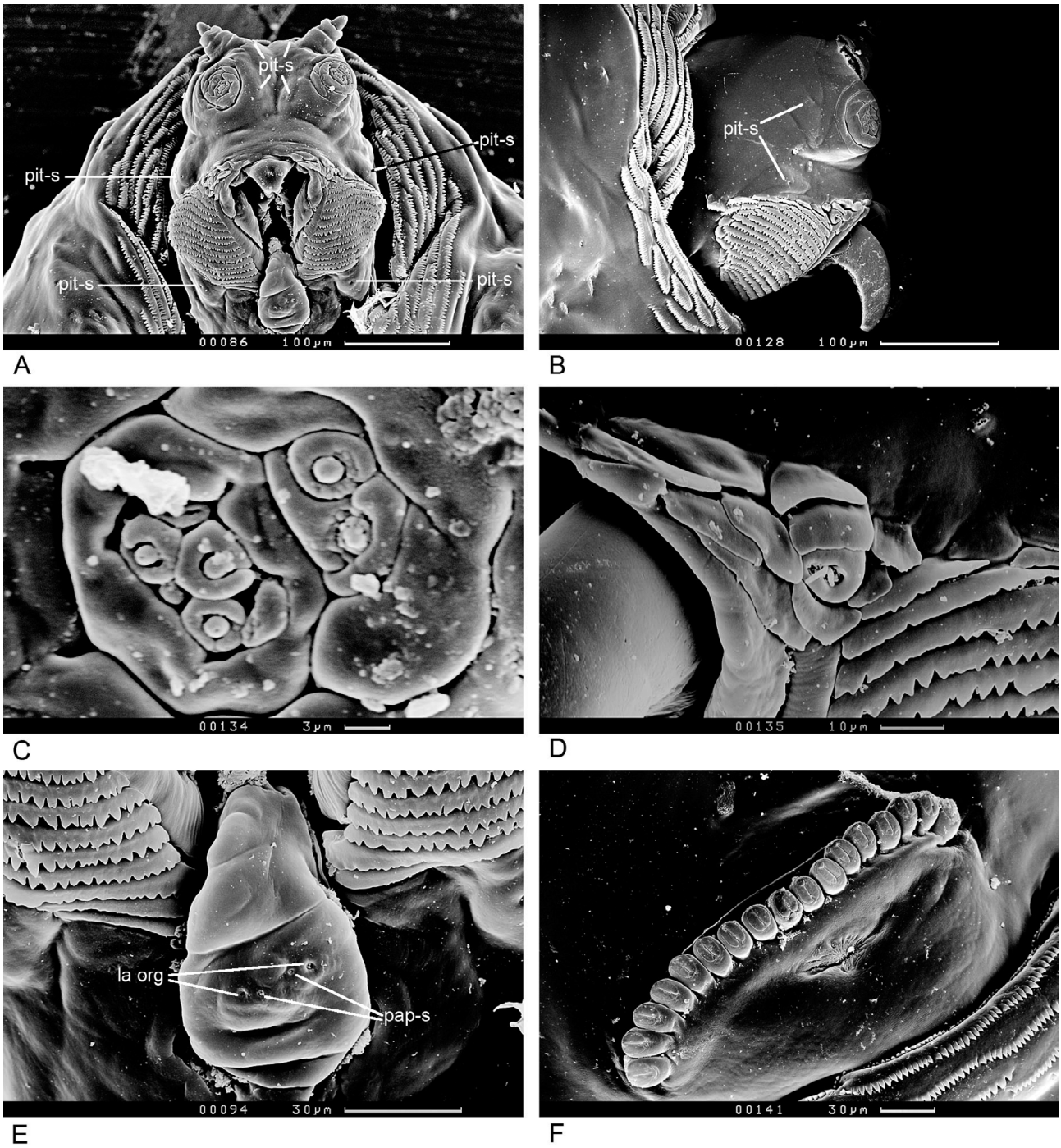

Fig. 13. Pseudocephalon and anterior spiracle of *Acroceratitis septemmaculata* (SEM micrographs). A – pseudocephalon, frontal view. B – pseudocephalon and part of the first thoracic segment, lateral view. C – maxillary sense organ. D – preoral organ located on primary preoral lobe, surrounded by remaining preoral lobes. E – labial lobe. F – anterior spiracle. Abbreviations: la org – labial organ, pap-s – papillar sensillum, pit-s – pit sensillum.

nodes lying next to each other. They devoured the wall substrate between sheath and pith ring (= the inner side of the culm wall composed of layers of often lignified parenchyma cells (Liese, 1998)) and usually did not enter the internode cavity (Fig. 12B). The largest number of larvae occurred in large upright shoots (more than 70 specimens), while in shoots lying on the ground the numbers were low. Young larvae were milky-pale, older larvae yellow, yellow-orange (orange especially in the front part) and at a later stage spotted yellow-green (Fig. 12C, D, E). Mature larvae readily skipped and left the internodes for pupariation. In three cases the development from egg-laying to eclosion of the adults lasted 20, 28 and 30 days.

Acroceratitis incompleta flies were recorded in the field between April and November. Females oviposited under sheaths in the upper part of larger shoots (base of zone Z1, Fig. 9A) belonging to *Dendrocalamus strictus* (Fig. 12F) and two additional undetermined *Dendrocalamus* spp.

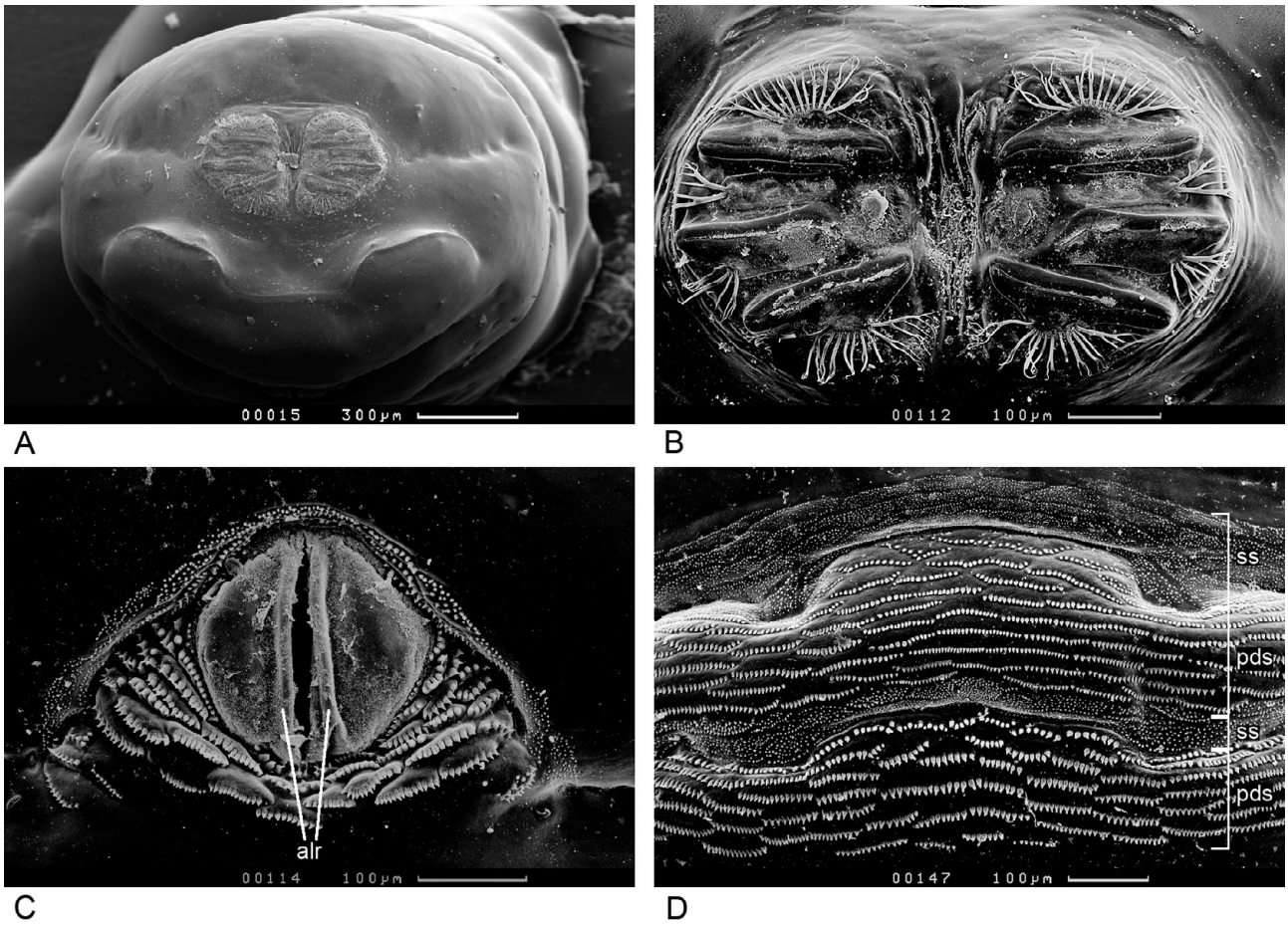

Fig. 14. Creeping welt and caudal segment showing the posterior spiracles and anus of *Acroceratitis septemmaculata* (SEM micrographs). A – caudal segment. B – posterior spiracles. C – anal lobes. D – creeping welt of fifth abdominal segment. Abbreviations: alr – anal lobe ridges, pds – posteriorly directed spinules, ss – small sensilla.

Acroceratitis septemmaculata Hardy, 1973

Description

As in *A. ceratitina*, except:

Habitus. Length: 8.0–10.1 mm (median: 9.6 mm; n = 11); maximum width: 1.6–1.8 mm (median: 1.7 mm; n = 11). Mature larvae broadest in the area of eighth abdominal segment, abdominal segments III–VII only slightly narrower.

Pseudocephalon (Fig. 13). Number of irregularly serrated oral ridges 15–20. With 12–16 serrated accessory plates.

Basal segment of antenna approximately cylindrical, apical segment cylindrical with rounded tip. Maxillary palpus surrounded by complete cuticular fold (Fig. 13C).

Primary preoral lobe rounded; number of preoral lobes 8–11 (Fig. 13D). Preoral organ bearing three peg and one pit sensilla. Surface of labial lobe entirely smooth (Fig. 13E).

Cephalopharyngeal skeleton (Fig. 16). Total length 0.8–1.2 mm (median: 1.0 mm; n = 11). Mouthhooks brown, indentation between apex of apical tooth and ventral apodeme 0.15–0.21× as deep as mouthhook length; apical tooth brown; neck well developed; preapical tooth 0.005–0.010 mm long; dorsal apodeme dorsally directed. Hypopharyngeal sclerite 2.9–4.4× as long as high, dark brown anterior, lighter brown posterior. Hypopharyngeal bridge 0.02–0.03 mm long and wide. Hyaline areas at posterior tips of both cornua, dorsal margin of dorsal cornu, and ventral margin of ventral cornu; light brown area of dorsal cornu slightly shorter than those of ventral cornu. Parastomal bars 0.89–1.07× as long as hypopharyngeal sclerite. Anterior sclerite present in 8 of 11 examined specimens.

Thorax. Anterior spiracles with 17–19 (in some cases flattened) tubules (Fig. 13F). Anterior margins of second and third thoracic segment lined with about 6 rows of spinules, on third thoracic segment all rows with a dorsal gap.

Abdominal segments I–VII. First abdominal creeping welt bearing about 9 rows of dentate plates; creeping welts of abdominal segments II–VII bearing rows of spinules arranged as follows (from anterior to posterior): A band of very small spinules, arranged in patches, 6–10 rows of medium sized, pointed, posteriorly directed spinules, a band of very small spinules, 4–7 rows of large, pointed, posteriorly directed spinules (Fig. 14D). Anterior margins of abdominal segments covered laterally by very small spinules.

Caudal segment (Figs 16 and 14A–C). Shortest distance between spiracles between one third and half as long as longest spiracular opening. Angle between dorsal and central opening up to 9°, shortest distance between dorsal and central opening about one third to half as long as

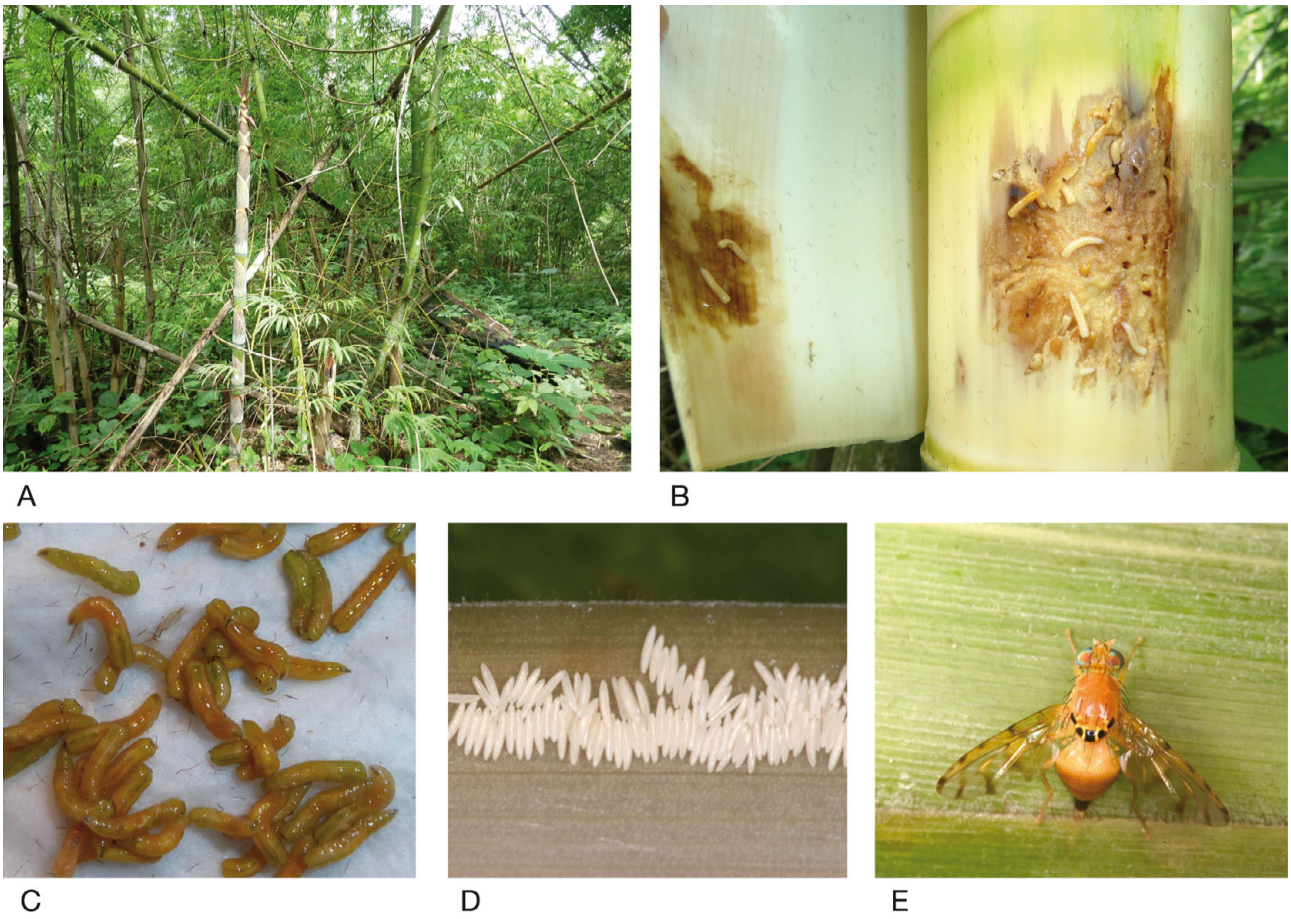

Fig. 15. Host plant, larvae and female of *A. septemmaculata*. A – large bamboo shoot of *Dendrocalamus strictus*, one of the host plants of *A. septemmaculata*. B – larvae boring on the surface and inside the internode wall of *D. strictus* (sheath partly removed). Younger larvae pale, older ones yellow. C – orange-green mature larvae. D – eggs of *A. septemmaculata* deposited on the underside of a culm sheath. E – female ovipositing under the sheath edge of *D. strictus*.

longest openings; angle between central and ventral opening 11–35°, shortest distance between central and ventral opening 0.1–0.4× as long as longest opening. Spiracular openings 6.3–9.2× as long as wide. Spiracular hairs up to somewhat more than one third as long as longest spiracular opening, branched up to 7×; dorsal bundle containing 7–20 hairs, ventral bundle containing 7–15 hairs, dorsolateral bundle containing 2–5 hairs, ventrolateral bundle containing 3–8 hairs (Figs 16 and 14B).

Anal lobes with ridge on each lobe. Patches of very small spinules anterior to anal lobes and 5–8 rows of dentate scales posterior to anal lobes (Fig. 14C). Creeping welt as in abdominal segments II–VII.

Puparium. Brown, 4.8–5.9 mm long (median: 5.6 mm; n = 5) and 1.8–2.4 mm wide (median: 2.3 mm; n = 5). Thoracic segments strongly tapering towards anterior end; abdominal segments more parallel sided, broadest at the third abdominal segment, slightly tapering towards posterior end.

Material examined. Thailand: North Thailand, Mae Hong Son, Pangmapha, near Soppong, larvae in shoot of *Dendrocalamus strictus*, 3.x.2010, sample Z31/2/2010b, 15 specimens, leg. D. Kovac.

Distribution. Thailand (Kovac et al., 2006).

Biology. So far, *A. septemmaculata* was reared from *Dendrocalamus strictus* (Dohm et al., 2014). In the present study *A. septemmaculata* was reared from living or freshly cut upright bamboo shoots of *Dendrocalamus strictus* (3×) and *Dendrocalamus* sp. (1×), cut side branches of a *D. strictus* shoot lying on the ground (1×) and a felled shoot of *Bambusa polymorpha* (1×). Larvae were found between July and November.

Most larvae were found in large shoots of *D. strictus* (Fig. 15A) and *D.* sp., which were about 2–3 m tall. Larvae developed at the base of zone Z1 and in the upper part of zone Z2 (Fig. 9A). They occupied 1–2 internodes lying next to each other. Larvae fed on the internode surface below the culm sheaths and then penetrated into the internode wall (Fig. 15B). One of the larger internodes contained more than 70 larvae. The color of younger *A. septemmaculata* larvae was pale yellow (Fig. 15B), older larvae turned yellow orange (orange more pronounced in the cephalic part of the body) and then spotted orange-green and greenish (Fig. 15C). Mature larvae readily skipped and left their internodes for pupariation.

Acroceratitis septemmaculata flies were recorded in the field between April and November. Eggs were laid side by side below internode sheaths (Fig. 15D). Females were observed to oviposit on *D. strictus* (Fig. 15E) and *D. ham-*

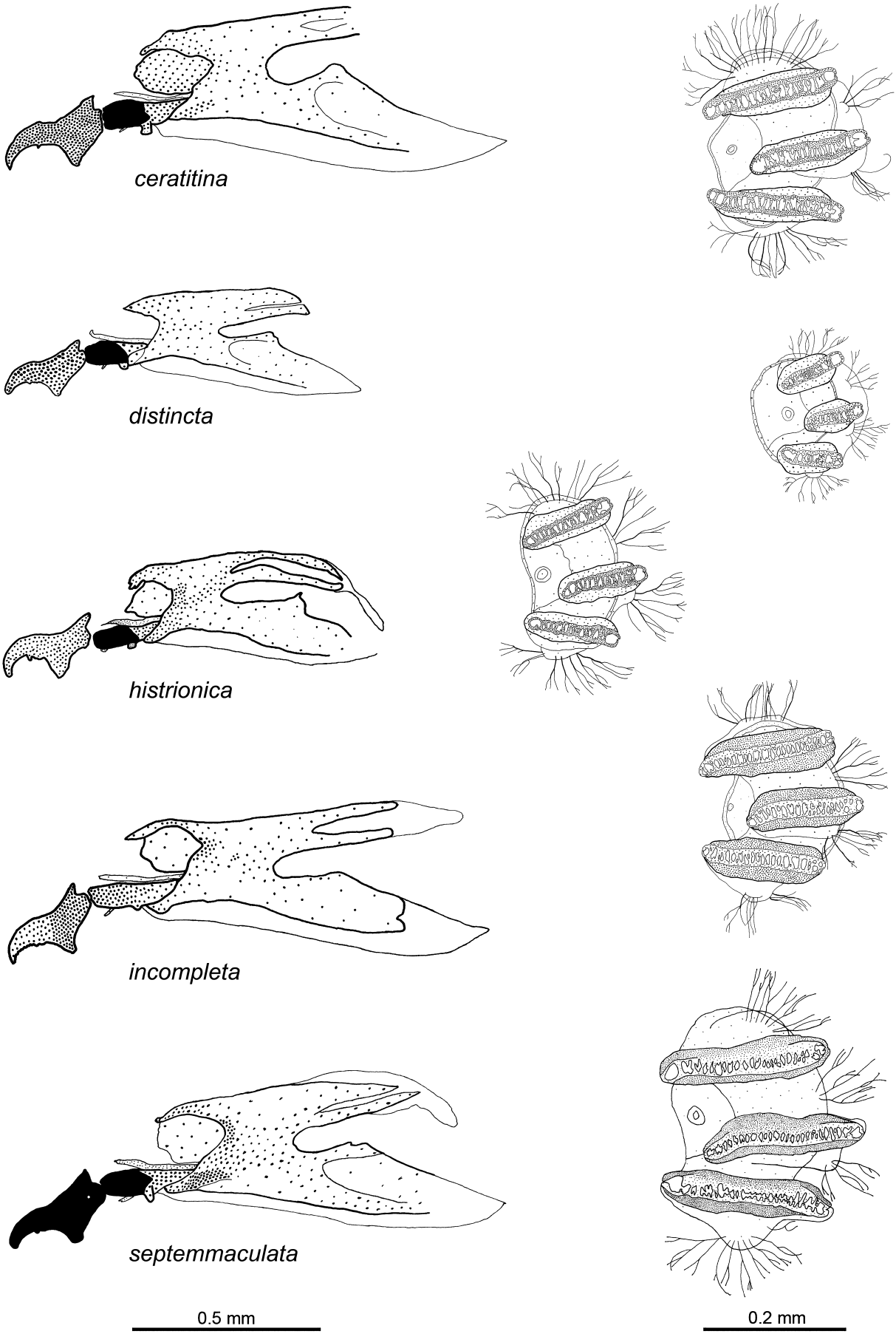

Fig. 16. Cephalopharyngeal skeleton (left) and posterior spiracle (right) of the third instar larvae of five *Acroceratitis* species investigated in the present study. All drawings to the same scale (cephalopharyngeal skeletons: 0.5 mm; posterior spiracles: 0.2 mm).

iltoni. Occasionally, two *A. septemmaculata* females laid their eggs side by side without interfering with one another.

DISCUSSION

Larval morphology

The facial masks of the examined *Acroceratitis* are approximately triangular and consist of moderately developed, serrated oral ridges, laterally surrounded by short, serrated accessory plates covering a much smaller area than the oral ridges. The facial mask of *Gastrozona fasciventris* is similar, but possesses dentate instead of serrated oral ridges (Elson-Harris, 1992: Plate 343). In other Gastrozonini the facial mask possesses dentate oral ridges with only a few accessory plates (*Cyrtostola limbata*; Elson-Harris, 1992: Plate 370), dentate oral ridges entirely lacking accessory plates (*Chaetellipsis*; Elson-Harris, 1992), possesses mostly accessory plates (*Ichneumonopsis burmensis*; Kovac et al., 2013) or is significantly reduced (*Acrotaeniostola spiralis*; Kovac et al., 2017).

The preoral organs of *Acroceratitis* are surrounded by very similarly structured non-serrated preoral lobes which are similar to *Chaetellipsis* (Elson-Harris, 1992: Plate 307) and *Gastrozona fasciventris* (Elson-Harris, 1992: Plates 341–343), however, they differ from those of *Cyrtostola limbata* (preoral lobes serrated) (Elson-Harris, 1992), *Acrotaeniostola spiralis* (different arrangement or reduced to various degrees) (Kovac et al., 2017) and *Ichneumonopsis burmensis* (preoral lobe surrounded by ordinary accessory plates) (Kovac et al., 2013).

The maxillary sense organs of *Acroceratitis* are similar to those of previously described Gastrozonini species. The antennae are two-segmented as in the third instar larvae of other described Gastrozonini larvae. In the basal area of the antennae there appears to be an additional antennal segment (see Figs 1A, B, 4A, B, 7A, B, 10, 10B, 13A). However, in our opinion this is most likely an artifact. This basal "segment" is, in contrast to the actual two antennal segments, rather amorphous, not well differentiated from the surface of the pseudocephalon, variable in size and shape or even not visible at all. For example, in one specimen of *Acrotaeniostola longicauda* the basal "segment" of one of the two antennae was not visible and there was just a deep furrow instead. In addition, the basal "segments" sometimes showed a transverse furrow at about the middle of their length. Therefore, the third basal "antennal segment" is probably just the invaginated base of the antenna, which protrudes from the pseudocephalon due to the heating process (see Material and methods). A similar third basal "antennal segment" is also visible in the SEM-micrographs presented by Elson-Harris (1992; Plates 312, 341). Nevertheless, she stated that there are only two antennal segments in the Gastrozonini larvae described by her (Elson-Harris, 1992).

The arrangement of pseudocephalic pit sensilla of *Acroceratitis* is identical to *Acrotaeniostola spiralis* and probably also to *Gastrozona fasciventris* (Elson-Harris, 1992: Plate 341 and 343, Kovac et al., 2017) and is probably the same in other Gastrozonini. However, in *Ichneumonopsis burmensis* and *Chaetellipsis maculosa* the isolated sensilla are located on pad-like lobes (= pad organ; Kovac et al., 2013) (Elson-Harris, 1992: Plate 312–314, Kovac et al., 2013).

The anterior spiracles of *Acroceratitis* consist of tubules arranged in a single row (Figs 1F, 4F, 7F, 10F, 13F). This arrangement was also found in *Chaetellipsis* and *Acrotaeniostola spiralis* (Elson-Harris, 1992, Kovac et al., 2017). In other Gastrozonini the tubules are arranged in two or more rows (*Cyrtostola limbata* and *Gastrozona fasciventris*; Elson-Harris, 1992) or the anterior spiracles consist of papillae arranged along radiating branches (*Ichneumonopsis burmensis*; Kovac et al., 2013).

All *Acroceratitis* species possess identical isolated sensilla on thoracic and abdominal larval segments (Fig. 17). SEM micrographs provided by Elson-Harris (1992) suggest that the sensilla of *Gastrozona fasciventris* are probably similarly arranged as in *Acroceratitis*. In contrast, *Acrotaeniostola spiralis* has an additional pit sensillum on the second and third thoracic segments and the sensillum number 11 on the first thoracic segment and number 10 on the third thoracic segment (counted dorsal to ventral) are pit sensilla instead of papilla sensilla, while *I. burmensis* has a significantly different arrangement (Kovac et al., 2013, 2017).

Caudal ridges (Figs 2A, 5A, 8A, 11A, 14A) and a dark transverse line (exception: rare specimens of *A. histrionica*, Table 1) are present in all *Acroceratitis* species. They are also present in *Chaetellipsis paradoxa*, *Cyrtostola limbata*, and *Gastrozona fasciventris* (own observations), but absent in *Ichneumonopsis burmensis* and *Acrotaeniostola spiralis* (Kovac et al., 2013, 2017).

Differences among the *Acroceratitis* species allow a division of the five species broadly into two groups. The first group consists of *Acroceratitis ceratitina*, *A. incompleta*, and *A. septemmaculata*. These three species have an additional pair of papillar sensilla on the labial lobe next to the labial organ (Figs 1E, 10E, 13E), lack large tubercles on the labial lobe, show a nearly identical pattern of spinules on the creeping welts (type 1; Figs 2D, 11D, 14D), and have a shorter distance between the posterior spiracles (up to about 0.5× the length of the longest spiracular opening). Larvae of *A. incompleta* and *A. septemmaculata* are very similar, while *A. ceratitina* shows some differences (labial lobe tubercles present, anal lobe ridges absent, posteriorly directed spinules posterior to anal lobes present, see Table 1).

The second group consists of *A. distincta* and *A. histrionica*. These species differ from the first group by the lack of additional papillar sensilla on labial lobe (Figs 4E, 7E), the presence of many large tubercles on labial lobe (Figs 4E, 7E), different arrangements of spinules on the creeping welts and a longer distance between the posterior spiracles (0.5–0.9× as long as the longest spiracular opening). *A. histrionica* and *A. distincta* are distinguished by different types of creeping welts. Furthermore, *A. histrionica* has fewer oral ridges, accessory plates and preoral lobes than *A. distincta*.

Table 1. Comparison of diagnostic characters of five *Acroceratitis* species (characters explained in the text). Abbreviations: ds – dentate scales, is – irregularly serrated, pds – posteriorly directed spinules, s – serrated.

Characters	*septemmaculata*	*incompleta*	*ceratitina*	*distincta*	*histrionica*
Oral ridges	15–20 (is)	14–16 (s)	19–22 (s)	13–14 (s)	7–9 (is)
Accessory plates	12–16	13–17	9–11	12–14	8–10
Preoral lobes	8–11	9–12	7–9	11–13	9–10
Labial lobe tubercles	absent	absent	few; small	many; large	many; large
Labial lobe sensilla	present	present	present	absent	absent
Anterior spiracle tubules	17–19	15–16	18–21	13–14	15–16
Creeping welt	type 1	type 1	type 1	type 2	type 3
Posterior spiracles (length / width)	6.3–9.2	6.7–9.4	6.7–7.8	4.0–6.0	5.4–7.3
Anal lobes ridges	present	present	absent	absent	absent
Spinules posterior to anal lobes	ds	ds	pds	pds	pds
Transverse line on caudal segment	present	present	present	present	present or absent

Biology

Acroceratitis larvae occupied specific bamboo niches depending on developmental stage and thickness of bamboo shoots, degree of protection by internode sheaths and condition of shoots (living or dead, placed in the upright position or lying on the ground). Thus, *A. ceratitina* occurred in thick young shoots just protruding from the ground (Fig. 3A, B), *A. incompleta* and *A. septemmaculata* in older and taller thick shoots (ca. 1.5 m or higher), *A. distincta* in thin shoots (Fig. 6A, B, C) and *A. histrionica* on surface of thick, older shoot internodes (Fig. 9A, C, D). Larvae inhabiting older (elongated) internodes always fed in the soft basal part of the internode, whereas the apical internode area was harder and sticking out from the protecting internode sheath.

Species mining in tall living shoots infested only 1–3 internodes per shoot, which were located in the apical shoot area (Fig. 6A). These internodes were probably particularly suitable for larval development, because they were softer than lower internodes and less protected by tight overlapping culm sheaths than apical internodes. *Acroceratitis histrionica* larvae were confined to living bamboo shoots, while other *Acroceratitis* developed successfully in living as well as in freshly cut shoots.

Freshly cut bamboo shoots were readily colonized by *A. ceratitina, A. incompleta* and *A. septemmaculata* when placed in the upright position, but larvae were lacking or rarely encountered in cut shoots lying on the ground. This is consistent with the observation that females were mainly walking on upright shoots in search of egg-laying sites. These findings indicate that females of these species used the vertical aspect of a bamboo shoot as visual cue for locating egg-laying sites.

The reason for the preference of upright shoots was perhaps the avoidance of competition with other Gastrozonini, especially *Gastrozona* and *Chaetellipsis*, because in large freshly cut shoots lying on the ground *Chaetellipsis* and *Gastrozona* were very common, while in upright cut shoots they were rarely found. Likewise, *Chaetellipsis* and *Gastrozona* were rarely found in thin living or cut shoots, while *A. distincta* larvae were abundant in living as well as in both vertical or horizontal cut shoots.

Acroceratitis histrionica larvae were special among *Acroceratitis*, because they developed on the surface of significantly hardened internode walls, rather than mining in the bamboo wall substrate (Fig. 9C, D). Nevertheless, their mouthparts did not differ from those of other *Acroceratitis*. Young *A. histrionica* larvae macerated the uppermost, soft layer of internode surface, while older larvae probably scraped food particles or microorganisms from the surface of underlying hard and fibrous internode wall.

Acroceratitis histrionica larvae developed in a triangular area ("feeding triangle") located close above the branch bud (Fig. 9C, D). Internodes lacking branch buds were not inhabited. The preference for the feeding triangle area was apparently not linked to the food quality at that location, since the internode surface looked identical on all sides of internode base and the branch bud was never eaten. It was rather connected to the fact that the growing branch bud pushed the corresponding culm sheath upward, thus producing a flat triangular cavity in which larvae could move around easily. Furthermore, moisture collected in the cavity, thus probably creating favorable microclimatic conditions for the larvae. On the other hand, occasional flooding of cavities led to periods of low oxygen and temporary immobility or even drowning of larvae.

Occasionally, freshly hatched *A. histrionica* larvae left indentations on the bamboo surface, thus allowing the reconstruction of the path towards their feeding site (Figs 9E, C, F). Judging from indentations the larvae chose the path of least resistance and squeezed downwards along the concealed sheath edge covered by the opposite end of the sheath. When reaching the basal internode area in the vicinity of the branch bud where the sheath was less tightly enclosing the internode surface larvae dispersed towards the feeding triangle area. In several cases indentations leading to the feeding triangle were present, but feeding marks were lacking, indicating that larvae had died for unknown reason.

Infested shoots showed different patterns of damage depending on *Acroceratitis* species. Small thick shoots attacked by *A. ceratitina* always died (Fig. 3A). Shoots infested by *A. distincta* remained alive and produced side branches, however, the apical part died off and fell to the ground (Figs 6A, B). *A. incompleta* and *A. septemmaculata* damaged the walls of 1–3 internodes of a particular shoot (Figs 12B, C, 15B), but it is not certain whether larvae killed the shoot or its apex. *A. histrionica* larvae damaged only small areas of the basal internode surfaces (Fig. 9F).

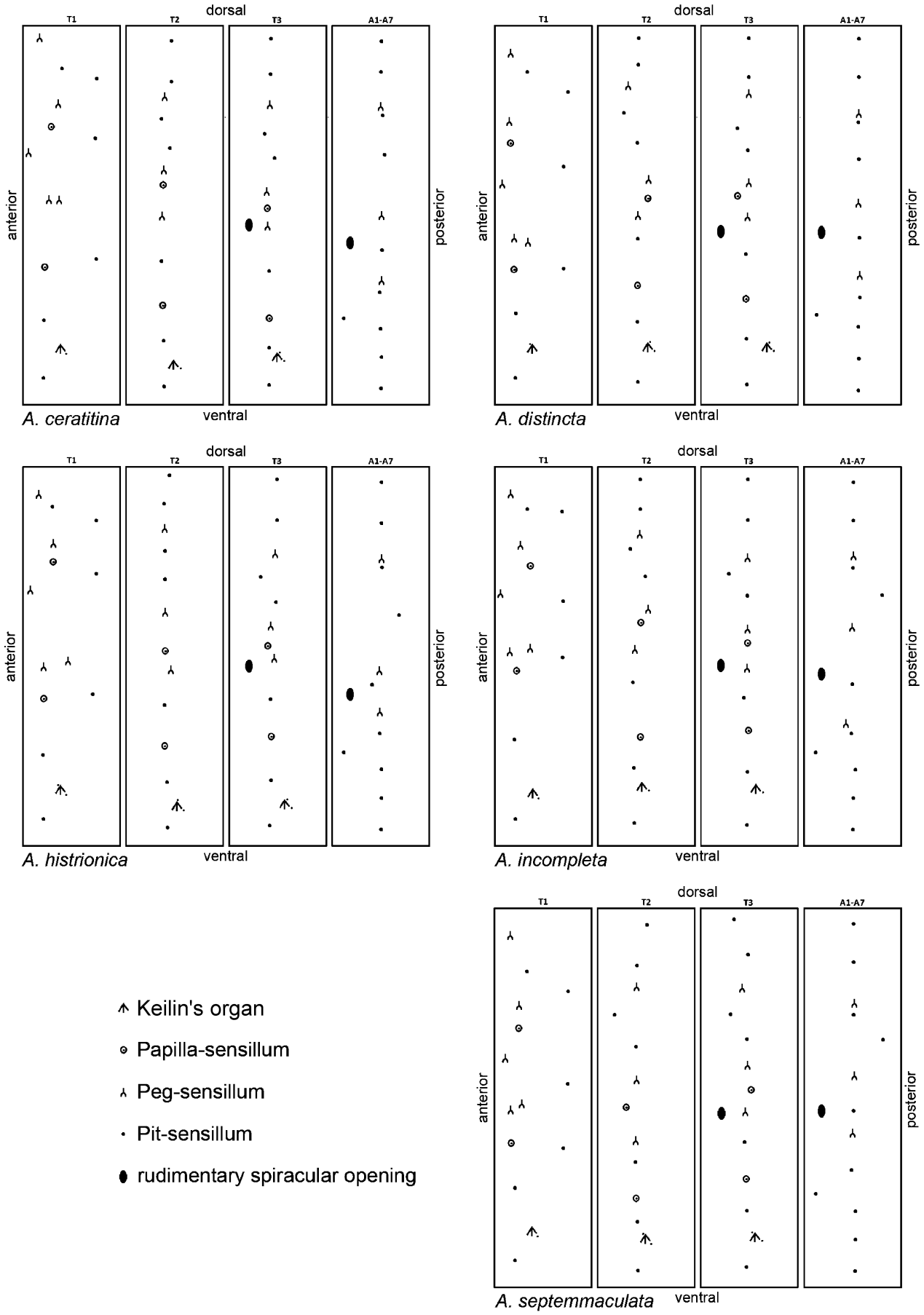

Fig. 17. Schematic illustration of the type and distribution of isolated sensilla on the thoracic and abdominal segments of five *Acroceratitis* species investigated in the present study. Abbreviations: A1–A7 – abdominal segments 1–7, T1, T2, T3 – thoracic segments 1, 2 and 3.

A. ceratitina larvae successfully penetrated cut shoots buried in the ground (Fig. 3B), but it is not certain whether they were able to overcome tight sheaths of intact bamboo shoots. According to present observations it is possible that *A. ceratitina* only infested shoots weakened by disease. Shoots killed by diseases (no traces of insect attacks) were common. They probably possessed slightly loosened shoots due to desiccation, thus allowing easier oviposition and access for *Acroceratitis*. This may also explain, why *A. incompleta* and *A. septemmaculata* larvae were more abundant in cut shoots placed in upright position rather than in intact living shoots. So far, only the Gastrozonini *Cyrtostola* and *Paraxarnuta* are known to overcome the apical sheaths barrier by using egg-laying holes made by *Cyrtotrachelus* beetles (Curculionidae) (Kovac & Azarae, 1994; Dohm et al., 2014).

The favorable response of flies to human urine and sweat was remarkable. It was probably triggered by ammonia, a breakdown product of urea which is also present in volatiles from fermentation of protein or bird droppings. Ammonia is a well-known attractant of fruit flies and is probably perceived by flies as a cue for a protein source (Bateman & Morton, 1981; Mazor et al., 1987; Thomas et al., 2008). In frugivorous tephritids and probably also in Gastrozonini protein feeding is essential for egg maturation, while it seems to be less important for males. However, in some species protein feeding may increase the reproductive success of males, for example, by increasing their pheromone production (overview in Drew & Yuval, 2000).

Studies with *Anastrepha* showed that urine-baited traps or fermenting protein lures tended to capture significantly more females than males, although the results varied with respect to previous diet, reproductive state, species, season and habitat (Piñero et al., 2002; Aluja & Piñero, 2004; Thomas et al., 2008). In the present study males of *A. distincta* were more frequent on sweat and urine than females (80 males and 5 females on sweat; 23 males and 1 female on urine). Other *Acroceratitis* showed the same trend, although the numbers of collected specimens were lower. This result indicates that protein feeding may be an essential factor for males of some *Acroceratitis* species.

Drew & Yuval (2000) postulated, that the relationship between male diet and reproductive success will be most pronounced in lekking species, where high levels of both protein and sugar are necessary for pheromone production, courtship displays and territory guarding. Lekking is present in Gastrozonini (Kovac, 2015), but the reproductive behavior of *Acroceratitis* remains to be investigated.

In summary, a comparison of morphological with biological data shows that *Acroceratitis* groups based on larval morphological characters coincide with differences in habitat or other factors like larval coloration. Thus, larvae of *A. ceratitina*, *A. incompleta* and *A. septemmaculata* developed in soft bamboo internodes and were orange-green to greenish when mature, while larvae of *A. distincta* and *A. histrionica* fed on elongated, harder shoot internodes and were bright yellow.

ACKNOWLEDGEMENTS. We thank D. Wiwatwitaya (Kasetsart University, Bangkok, Thailand) and the Florida Department of Agriculture and Consumer Services – Division of Plant Industry for their support of this contribution, and we are grateful to E. Junqueira for preparing Figs 6, 9, 12 and 15.

REFERENCES

Allwood A.J., Chinajariyawong A., Kritsaneepaiboon S., Drew R.A.I., Hamacek E.L., Hancock D.L., Hengsawad C., Jipanin J.C., Jirasurat M., Krong C.K., Leong C.T.S. & Vijaysegaran S. 1999: Host plant records for fruit flies (Diptera: Tephritidae) in Southeast Asia. — *Rafft. Bull. Zool.* **47**(Suppl. No. 7): 1–92.

Aluja M. & Piñero J. 2004: Testing human urine as a low-tech bait for *Anastrepha* spp. (Diptera: Tephritidae) in small guava, mango, sapodilla and grapefruit orchards. — *Fla Entomol.* **87**: 41–50.

Bateman M.A. & Morton T.C. 1981: The importance of ammonia in proteinaceous attractants for fruit flies (Diptera: Tephritidae). — *Austral. J. Agric. Res.* **32**: 883–903.

Carroll L.E. 1992: *Systematics of Fruit Fly Larvae (Diptera: Tephritidae)*. Unpubl. PhD thesis, Texas A&M University, College Station, TX, 341 pp.

Copeland R.S. 2007: On the occurrence of *Bistrispinaria*, grass-breeding fruit flies (Diptera, Tephritidae), in Kenya, with an addition to the tephritid checklist of Kakamega forest. — *J. East Afr. Nat. Hist.* **96**: 95–102.

Courtney G.W., Sinclair B.J. & Meier R. 2000: 1.4. Morphology and terminology of Diptera larvae. In Papp L. & Darvas B. (eds): *Contributions to a Manual of Palearctic Diptera, Vol. 1. General and Applied Dipterology.* Science Herald, Budapest, pp. 85–162.

David K.J., Hancock D.L. & Ramani S. 2014: Two new species of *Acroceratitis* Hendel (Diptera: Tephritidae) and an updated key for the species from India. — *Zootaxa* **3895**: 411–418.

Dohm P., Kovac D., Freidberg A., Rull J. & Aluja M. 2014: Basic biology and host use patterns of tephritid flies (Phytalminae: Acanthonevrini, Dacinae: Gastrozonini) breeding in bamboo (Poaceae: Bambusoidea). — *Ann. Entomol. Soc. Am.* **107**: 184–203.

Drew R.A.I. & Yuval B. 2000: The evolution of fruit fly feeding behavior. In Aluja M. & Norrbom A.L. (eds): *Fruit Flies (Tephritidae): Phylogeny and Evolution of Behavior*. CRC Press, London, pp. 731–749.

Elson-Harris M.M. 1992: *A Systematic Study of Tephritidae (Diptera) Based on the Comparative Morphology of Larvae.* Unpubl. PhD thesis, University of Queensland, Brisbane, Vol. 1: xvi + 314 pp., Vol. 2: xi + 52 pp.

Frías D., Hernández-Ortiz V., Vaccaro N.C., Bartolucci A.F. & Salles L.A. 2006: Comparative morphology of immature stages of some frugivorous species of fruit flies (Diptera: Tephritidae). — *Isr. J. Entomol.* **35–36**: 423–457.

Frías Lasserre D., Hernández-Ortiz V. & López-Munoz L. 2009: Description of the third-instar of *Anastrepha leptozona* Hendel (Diptera: Tephritidae). — *Neotrop. Entomol.* **38**: 491–496.

Gardner S., Sidisunthorn P. & Anusarnsunthorn V. 2000: *A Field Guide to Forest Trees of Northern Thailand*. Kobfai Publishing Projekt, Bangkok, xiv + 545 pp.

Hancock D.L. 1999: Grass-breeding fruit flies and their allies of Africa and Asia (Diptera: Tephritidae: Ceratitidinae). — *J. Nat. Hist.* **33**: 911–948.

Hancock D.L. & Drew R.A.I. 1999: Bamboo-shoot fruit flies of Asia (Diptera: Tephritidae: Ceratitidinae). — *J. Nat. Hist.* **33**: 633–775.

Korneyev V.A. 1999: Phylogenetic relationships among higher groups of Tephritidae. In Aluja M. & Norrbom A.L. (eds): *Fruit Flies (Tephritidae): Phylogeny and Evolution of Behavior*. CRC Press, London, pp. 73–113.

Kovac D. 2015: Reproductive behavior and basic biology of the Oriental bamboo-inhabiting *Anoplomus rufipes* and a comparison with frugivorous Dacinae fruit flies. — *Insects* **6**: 869–896.

Kovac D & Azarae I. 1994: Depredations [sic] of a bamboo shoot weevil: an investigation. — *Nature Malays.* **19**: 115–122.

Kovac D., Dohm P., Freidberg A. & Norrbom A.L. 2006: Catalog and revised classification of the Gastrozonini (Diptera: Tephritidae: Dacinae). — *Isr. J. Entomol.* **35–36**: 163–196.

Kovac D., Freidberg A. & Steck G.J. 2013: Biology and description of the third instar larva and puparium of *Ichneumonopsis burmensis* Hardy (Diptera: Tephritidae: Dacinae: Gastrozonini), a bamboo-breeding fruit fly from the Oriental Region. — *Raffles Bull. Zool.* **61**: 117–132.

Kovac D., Schneider A., Freidberg A. & Wiwatwitaya D. 2017: Life history and description of the larva of *Acrotaeniostola spiralis* (Diptera: Tephritidae: Dacinae: Gastrozonini), an Oriental fruit fly inhabiting bamboo twigs. — *Raffles Bull. Zool.* **65**: 154–167.

Liese W. 1998: *The Anatomy of Bamboo Culms: Technical Report 18*. International Network for Bamboo and Rattan, Beijing, 208 pp.

Nation J.L. 1983: A new method using hexamethyldisilazane for preparation of soft insect tissues for scanning electron microscopy. — *Stain Technol.* **58**: 347–351.

Mazor M., Gothilf S. & Galun R. 1987: The role of ammonia in the attraction of females of the Mediterranean fruit fly to protein hydrolysate baits. — *Entomol. Exp. Appl.* **43**: 25–29.

Müller J.M. 1996: Handbuch ausgewählter Klimastationen der Erde. 5th Ed. Universität Trier, Trier, 400 pp.

Piñero J., Aluja M., Equihua M. & Ojeda M.M. 2002: Feeding history, age and sex influence the response of four economically important *Anastrepha* species (Diptera: Tephritidae) to human urine and hydrolyzed protein. — *Folia Entomol. Mexic.* **41**: 283–298.

Steck G.J. & Wharton R.A. 1986: Descriptions of immature stages of *Eutreta* (Diptera, Tephritidae). — *J. Kans. Entomol. Soc.* **59**: 296–302.

Steck G.J., Carroll L.E., Celedonio-Hurtado H. & Guillen-Aguilar J. 1990: Methods for identification of *Anastrepha* larvae (Diptera, Tephritidae), and key to thirteen species. — *Proc. Entomol. Soc. Wash.* **92**: 333–346.

Thomas D.B., Epsky N.D., Kendra P.E., Heath R.A., Serra C. A. & Hall D.G. 2008: Ammonia formulations and capture of *Anastrepha* fruit flies (Diptera: Tephritidae). — *J. Entomol. Sci.* **43**: 76–85.

White I.M. & Elson-Harris M.M. 1992: *Fruit Flies of Economic Significance: Their Identification and Bionomics*. CAB International, Wallingford, 601 pp.

White I.M., Headrick D.H., Norrbom A.L. & Carroll L.E. 1999: 33 Glossary. In Aluja M. & Norrbom A.L. (eds): *Fruit Flies (Tephritidae): Phylogeny and Evolution of Behavior*. CRC Press, London, pp. 881–924.

Yu H., Deng Y.-L., He W.-Z., Liu Z.-S., Yang D. & Chen N.-Z. 2010: A new record of the Tephritidae (Diptera) from Yunnan, China. — *Entomotaxonomia* **32**: 289–292.

Received July 13, 2017; revised and accepted August 22, 2018
Published online October 11, 2018